

2

NAVAL POSTGRADUATE SCHOOL

Monterey, California

AD-A246 997



DTIC
SELECTE
MAR 06 1992
S B D

THESIS

BACKPROPAGATION NEURAL NETWORK FOR
NOISE CANCELLATION APPLIED TO THE NUWES
TEST RANGES

by

Charles H Wellington Jr.

December 1991

Thesis Advisor:

Murali Tummala

Approved for public release; distribution is unlimited.

92 3 03 280

92-05725



UNCLASSIFIED

SECURITY CLASSIFICATION OF THIS PAGE

REPORT DOCUMENTATION PAGE				Form Approved OMB No. 0704-0188	
1a. REPORT SECURITY CLASSIFICATION UNCLASSIFIED			1b. RESTRICTIVE MARKINGS		
2a. SECURITY CLASSIFICATION AUTHORITY			3. DISTRIBUTION AVAILABILITY OF REPORT Approved for public release; distribution is unlimited		
2b. DECLASSIFICATION/DOWNGRADING SCHEDULE					
4. PERFORMING ORGANIZATION REPORT NUMBER(S)			5. MONITORING ORGANIZATION REPORT NUMBER(S)		
6a. NAME OF PERFORMING ORGANIZATION Naval Postgraduate School		6b. OFFICE SYMBOL (If applicable) EC		7a. NAME OF MONITORING ORGANIZATION Naval Postgraduate School	
6c. ADDRESS (City, State, and ZIP Code) Monterey, California 93943-5000			7b. ADDRESS (City, State, and ZIP Code) Monterey, California 93943-5000		
8a. NAME OF FUNDING SPONSORING ORGANIZATION		8b. OFFICE SYMBOL (If applicable)		9. PROCUREMENT INSTRUMENT IDENTIFICATION NUMBER	
8c. ADDRESS (City, State, and ZIP Code)			10. SUBJECT TERMS		
			PROGRAM ELEMENT NO. PROJECT NO. TASK NO. INTER-UNIT ACCESSION NO.		
11. TITLE (Include Security Classification) Backpropagation Neural Network for Noise Cancellation Applied to the NUWES Test Ranges					
12. PERSONAL AUTHOR Charles H. Wellington Jr					
13a. TYPE OF REPORT Thesis, M.S.		13b. TIME COVERED FROM TO		14. DATE OF REPORT (Year, Month, Day) December, 1991	
15. PAGE COUNT 77					
16. SUPPLEMENTARY NOTES The views expressed in this thesis are those of the author and do not reflect the official policy or position of the Department of Defense or the U.S. Government.					
17. CUSC (Circle)			18. SUBJECT TERMS (Continue on reverse if necessary and identify by block number)		
FIELD	GROUP	SUBJECT	Backpropagation neural networks		
19. ABSTRACT (Continue on reverse if necessary and identify by block number) This thesis investigates the application of backpropagation neural networks as an alternative to adaptive filtering at the NUWES test ranges. To facilitate the investigation, a model of the test range is developed. This model accounts for acoustic transmission losses, the effects of doppler shift, multipath, and finite propagation times delay. After describing the model, the backpropagation neural network algorithm and feature selection for the network are explained. Then, two schemes based on the network's output, signal waveform recovery, and binary code recovery are applied to the model. Simulation results of the signal waveform recovery and direct code recovery schemes are presented for several scenarios.					
20. DISTRIBUTION AVAILABILITY STATEMENT <input checked="" type="checkbox"/> UNCLASSIFIED/UNLIMITED <input type="checkbox"/> SAME AS REPORT <input type="checkbox"/> OTHER			21. ABSTRACT SECURITY CLASSIFICATION UNCLASSIFIED		
22. NAME OF PERSON/ORGANIZATION Professor Murali Tummala			23. TELEPHONE (Include Area Code) 408-646-2645		

DD Form 1473, JUN 86

Previous editions are obsolete.

S/N 0101-25-014-6003

UNCLASSIFIED

Approved for public release: distribution is unlimited

BACKPROPAGATION NEURAL NETWORK FOR NOISE CANCELLATION
APPLIED TO THE NUWES TEST RANGES

by

Charles H. Wellington Jr.
Lieutenant, United States Navy
B.S.E.E., University of Idaho, (1986)

Submitted in partial fulfillment
of the requirements for the degree of

MASTER OF SCIENCE IN ELECTRICAL ENGINEERING

from the

NAVAL POSTGRADUATE SCHOOL

December 1991

Author:

Charles H. Wellington Jr.

Charles H. Wellington Jr

Approved by:

Murali Tummala

Murali Tummala, Thesis Advisor

Harold A. Titus

Harold A. Titus, Second Reader

Michael A. Morgan

Michael A. Morgan, Chairman

Department of Electrical and Computer Engineering

ABSTRACT

This thesis investigates the application of backpropagation neural networks as an alternative to adaptive filtering at the NUWES test ranges. To facilitate the investigation, a model of the test range is developed. This model accounts for acoustic transmission losses, the effects of doppler shift, multipath, and finite propagation time delay. After describing the model, the backpropagation neural network algorithm and feature selection for the network are explained. Then, two schemes based on the network's output, signal waveform recovery and binary code recovery, are applied to the model. Simulation results of the signal waveform recovery and direct code recovery schemes are presented for several scenarios.



Accession For	
NTIS GRA&I	<input checked="checked" type="checkbox"/>
DTIC TAB	<input type="checkbox"/>
Unannounced	<input type="checkbox"/>
Justification	
By	
Distribution/	
Availability Codes	
Dist	Avail and/or Special
A-1	

TABLE OF CONTENTS

I. INTRODUCTION	1
A. OBJECTIVE	1
B. ORGANIZATION	1
II. PROBLEM DESCRIPTION	3
A. INTRODUCTION	3
B. SIGNAL AND COUNTERMEASURE PARAMETERS	3
C. RANGE DESCRIPTION	4
D. SIGNAL MODEL	6
1. Acoustic Losses	7
2. Doppler Effect	9
3. Multipath	10
4. Hydrophone	10
III. BACKPROPAGATION NEURAL NETWORK	12
A. INTRODUCTION	12
B. BACKPROPAGATION THEORY	12
C. SOLUTION	18

IV. SIMULATION RESULTS	20
A. INTRODUCTION	20
B. BANDPASS RESULTS	20
1. Signal Waveform Recovery	21
2. Binary Code Recovery	22
C. BASEBAND RESULTS	30
 V. CONCLUSIONS AND RECOMMENDATIONS	36
A. CONCLUSIONS	36
B. RECOMMENDATIONS	37
 APPENDIX A	38
APPENDIX B	46
LIST OF REFERENCES	66
INITIAL DISTRIBUTION LIST	67

LIST OF FIGURES

2.1 Map showing array representation for Nanoose Range. A sensor platform is located at the center of each circle.	5
2.2 Hydrophone arrangement for sensor platforms at Nanoose Range	6
2.3 Acoustic paths from torpedo and countermeasure to sensor platform hydrophones	8
2.4 Frequency response of simulated hydrophone using a 12 th order Butterworth Filter	10
2.5 Actual frequency response of hydrophones used at Nanoose Range	11
3.1 Perceptron Model	13
3.2 Examples of nonlinear functions used to modify the output of a given processing element	14
3.3 Backpropagation Network with input, output and one hidden layer	15
3.4 Schematic diagram of general solution model.	18
4.1 Model for direct signal recovery in the bandpass region	21
4.2 (a) Signal input to the hydrophone and power spectrum. (b) Signal input to FFT and power spectrum. (c) Processed signal output and power spectrum.	23
4.3 Model for direct code recovery in the bandpass region	24
4.4 Network performance after each training stage for the Four Bit	

Direct Recovery Network.	25
4.5 Multipath vs. Direct path propagation of Countermeasure noise	27
4.6 Monte Carlo simulations with various phase delays	29
4.7 Model for direct code recovery in the baseband region.	30
4.8 Network performance after each training stage for the Four	
Bit Direct Recovery Network in the baseband region	32
4.9 Doppler effects with sampling rate held constant	33
4.10 Doppler effects for constant four time oversampling rate	34

INTRODUCTION

A. OBJECTIVE

The Naval Undersea Warfare Engineering Station (NUWES) is currently conducting tests, at the Nanoose range, with torpedoes and broadband countermeasures. Prior to each test, a transponder is attached to the torpedo to transmit telemetry data during the test, which is then received by a set of hydrophones mounted on the ocean floor. The received signal is then processed by onshore computers located at Winchelsea Island Computer Center. However, noise from the broadband countermeasure interferes with the recovery of this information. This thesis investigates the use of neural networks to recover the signals emitted by the attached transponder in broadband countermeasure noise.

B. ORGANIZATION

The thesis contains five chapters and two appendices. Chapter II presents a more detailed description of the problem and the test range currently in use. Model parameters used to model the signal, noise, and the range are also presented. Chapter III gives a brief explanation of the backpropagation neural network algorithm and presents a generalized solution. Chapter IV presents simulation results and specific details amplifying the general solution described in Chapter III. Chapter V contains conclusions and recommendations. Two appendices are also

provided. Appendix A contains a listing of the programs used to generate training data sets and Monte Carlo simulations. Appendix B provides a listing of interconnection weights developed for one neural network.

II. PROBLEM DESCRIPTION

A. INTRODUCTION

In range testing the torpedo telemetry data, referred to as the tracking signal hereafter, is severely corrupted by the wideband countermeasure noise. Consequently the recovery of the tracking signal is very difficult, especially when the test vehicle is in close proximity to the countermeasure. NUWES is seeking efficient signal processing methods to improve reception of torpedo telemetry data. This research examines the performance of neural network algorithms, based on the well known backpropagation method, to extract the transmitted telemetry data from the received signal in the presence of broadband countermeasure noise.

B. SIGNAL AND COUNTERMEASURE PARAMETERS

A transponder is attached to the torpedo prior to range testing. The transponder transmits pulses at a frequency of 75 kHz in discrete time intervals. The entire torpedo telemetry code, which is in the binary form, consists of 48 bits: 19 bits used as an object identifier, 28 bits for data telemetry, and one parity bit. This information is modulated on to the 75 kHz carrier frequency using a binary phase shift keyed (BPSK) technique. Each bit occupies seven cycles of the 75 kHz carrier frequency.

For optimal signal recovery performance, the BPSK signal must be sent in an environment supporting direct path without strong reflected paths [Ref. 1]. Since reflected paths may occur during any test, they must be eliminated as much as possible. However, the telemetry information is transmitted at discrete time intervals and the reflected signal is typically received in an interval that does not overlap with the time interval in which the direct path signal is recovered. Thus, after receipt of the direct path signal, the subsequent reflected path signals can be identified and safely ignored.

Countermeasure generated acoustic noise is constantly present at the receiver input and is the primary source of noise. The broadband countermeasure noise is modeled as gaussian white noise. Additional noise may arrive at the receiver from surface reflections when such reflections are supported by the acoustic environment. In addition, the Doppler shift created by movement of the torpedo affects the signal spectrum as a function of the relative motion between transmitter and receiver.

C. RANGE DESCRIPTION

Nanoose Range is a deep water range with hydrophone sensor platforms mounted on the bottom and spaced approximately 2000 yards apart. Figure 2.1 shows the range array configuration. Overlapping coverage of sensor platforms allows continuous tracking of the torpedo. The range has a sandy bottom, thus reducing bottom bounce. Nanoose Range has been designed to use short baseline sensor platforms. Each sensor platform is a small array with four hydrophones spaced

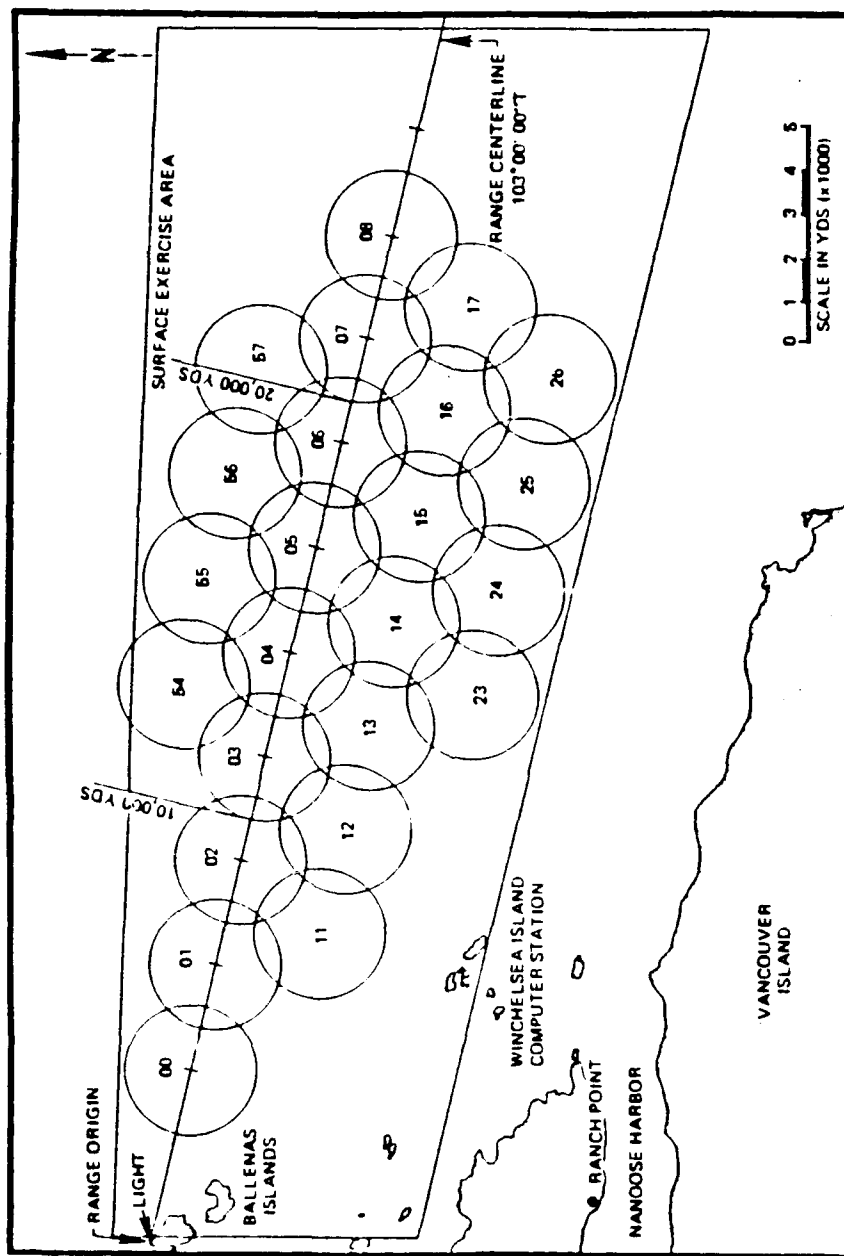


Figure 2.1 Map showing array representation for Nanoose Range. A sensor platform is located at the center of each circle.

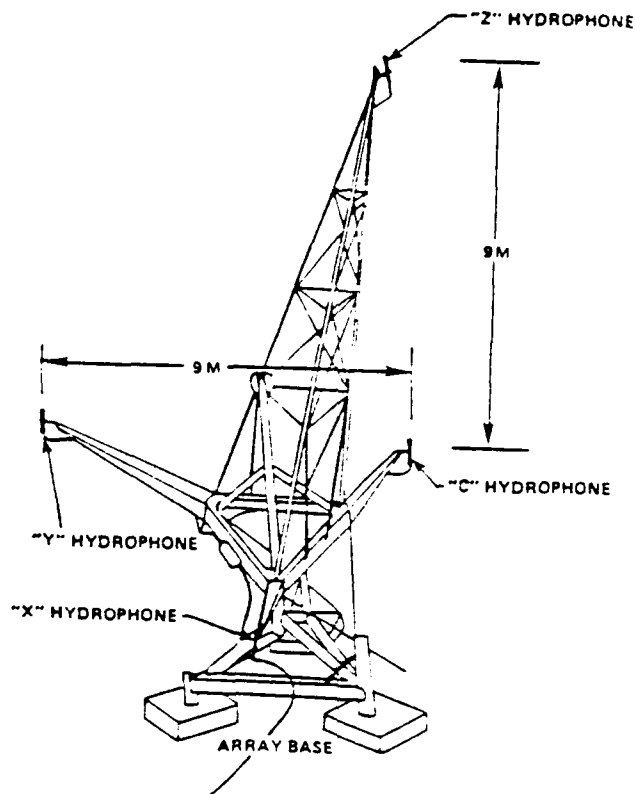


Figure 2.2 Hydrophone arrangement for sensor platforms at Nanoose Range.

nine meters apart. Figure 2.2 shows the hydrophone arrangement for each sensor platform. Multiple hydrophones at each sensor permit vehicle tracking in three dimensions along with the reception of telemetry data. The BPSK signal is the primary method for transmitting telemetry data on the Nanoose Range.

D. SIGNAL MODEL

The torpedo or tracking signal carrying data is a 75 kHz BPSK waveform transmitted at discrete intervals of time where each pulse contains a 48 bit binary code. Each bit lasts $93 \mu\text{s}$, resulting in a signal bandwidth of approximately 20 kHz. The telemetry signal in noise can be represented as

$$x(n) = \pm A \cos\left(\frac{2\pi f_c n}{f_s}\right) + N(n) \quad (2.1)$$

where $f_c = 75$ kHz is the carrier frequency, $f_s = 300$ kHz is the sampling frequency, A is the magnitude of a square wave representing the binary code used in this study, and $N(n)$ represents the additive countermeasure noise. Assumed ambient noise is typically at levels much less than that of the signal or countermeasure noise, and is not included in the model.

1. Acoustic Losses

The acoustic environment model used contains the following simplifying assumptions. First, sound propagation is approximated by Ray theory. Second, an Isospeed sound channel with a sound velocity c of 1500 m/s (4900 ft/s) allows both signal and noise to travel in straight line paths. Finally, no bottom reflection is allowed, since the sensor platform is mounted on the bottom. Surface reflection of both tracking signal and countermeasure noise are included in the model. However, multiple reflections from surface and bottom are not included. Figure 2.3 shows several typical paths from the transmitter to the receiver based on the criteria above.

Transmission losses occur from spreading and absorption of the signal. Spreading losses vary logarithmically with range [Ref. 9:pp.99-103] and absorption losses vary logarithmically with frequency [Ref. 10:p.100]. For a fixed frequency the absorption loss is linear. At frequencies above 10 kHz, the attenuation of signals due

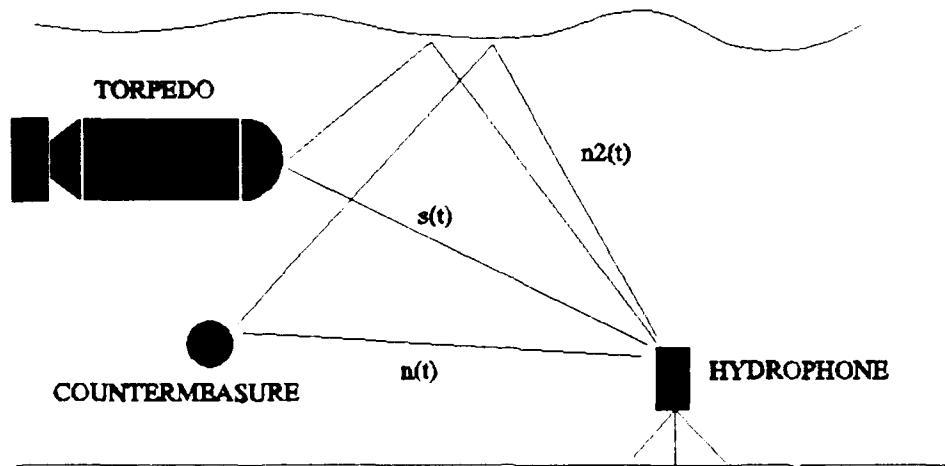


Figure 2.3 Acoustic paths from torpedo and countermeasure to sensor platform hydrophones.

to absorption becomes significant. Both these losses may be combined and represented as the transmission loss

$$TL = 20 \log_{10} R + \alpha' R \text{ dB} \quad (2.2)$$

where R is the range from the transmitter source to the receiver and α' is the absorption coefficient. For the carrier frequency of 75 kHz, α' is approximately 0.04 [Ref 10]. Equation 2.2 shows that spreading losses dominate for a range of less than 1000 yards and absorption losses dominate for R greater than 1000 yards.

To simplify the simulation, the transmitted BPSK signal amplitude at the receiving hydrophone is assumed to have unit magnitude, i.e., $A = \pm 1$. The Signal to Noise Ratio (SNR) is defined as

$$SNR = 10 \log_{10} \left(\frac{E[x^2(n)]}{\sigma^2} \right) \quad (2.3)$$

where $E[x^2(n)]$ is signal power, and σ^2 is the countermeasure noise average power.

2. Doppler Effect

Since the transmitting torpedo is constantly moving and since ocean currents may cause movement in the countermeasure, doppler shift must be considered as the signal model is developed. The doppler change in frequency caused by torpedo motion is:

$$\Delta f = \frac{2v}{c} f \text{ Hz} \quad (2.4)$$

where v is relative velocity between the transmitter and receiving sensor platform, f is the operating frequency of the transmitter and c is the velocity of sound set at 4900 ft/s (1500 m/s). For transmission purposes, during any given range test, c is considered constant. For a sound velocity of 4,900 ft/s and a carrier frequency of 75 kHz, Equation (2.4) reduces to $\Delta f = \pm 51.75 \text{ Hz/knot}$.

Typical ocean currents at the Nanoose range appear to be five knots. This current changes the effective torpedo speed and also causes some movement of the countermeasure source platform. To facilitate examination of doppler effect, the maximum speed of the test torpedo is limited to fifty knots. Since the torpedo's

maximum operating speed is assumed to be much greater than the speed of existing ocean currents, the doppler shift from the countermeasure is neglected in this study.

3. Multipath

Signals arriving at a receiver array from multiple paths may have constructive or destructive interference. Since the hydrophones are bottom mounted, only the effects from surface reflections are considered here. Since an isospeed sound channel is assumed, arrivals via surface reflection are simply modeled as attenuated, time-delayed versions of the direct path waveforms.

4. Hydrophone

The hydrophone and preamplifier combination has a frequency response which is bandlimited and centered around 75kHz. This frequency response is simulated in the model by a 12th order Butterworth filter. Figure 2.4 shows the frequency response of the simulated hydrophone sensor while Figure 2.5 shows the actual frequency response. The two responses closely resemble each other.

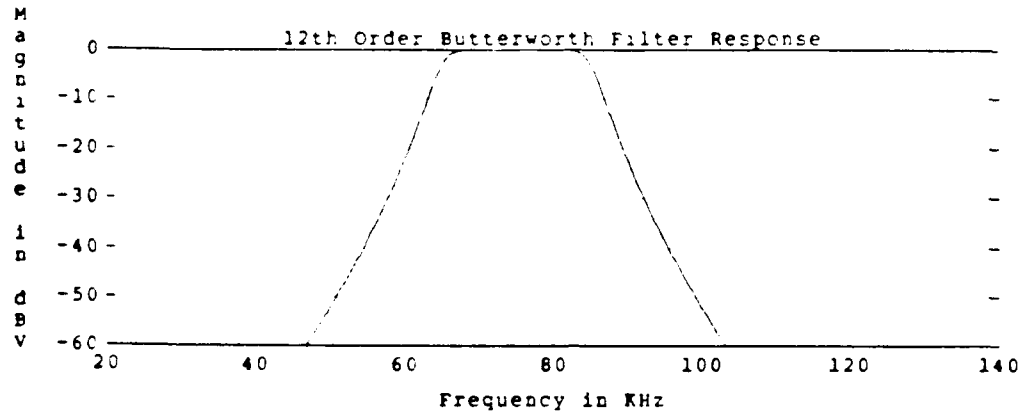


Figure 2.4 Frequency response of simulated hydrophone using a 12th order Butterworth Filter.

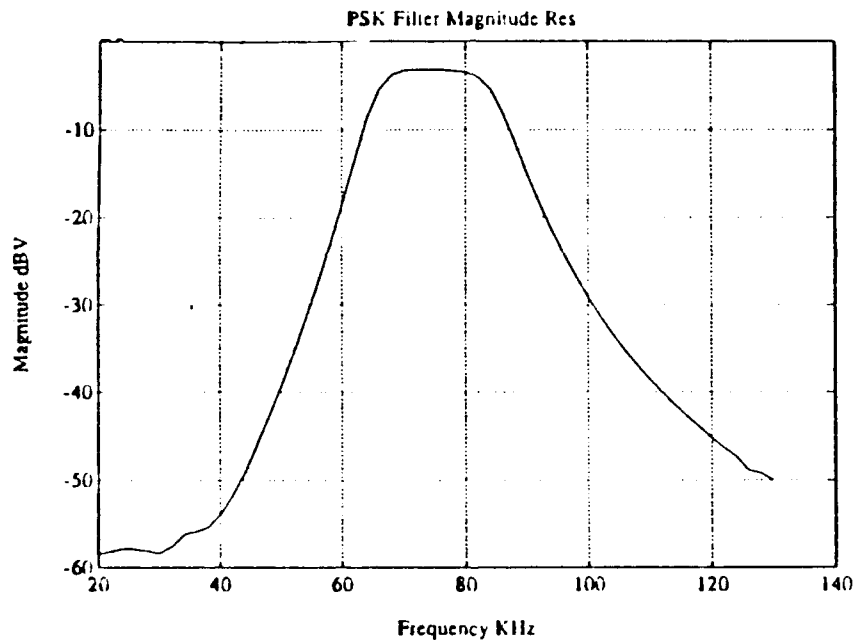


Figure 2.5 Actual frequency response of hydrophones used at Nanoose Range.

III BACKPROPAGATION NEURAL NETWORK

A. INTRODUCTION

An algorithm for extracting a desired signal in noise can be viewed as one that recognizes a pattern or series of patterns corresponding to the signal and suppresses all undesired patterns, those corresponding to noise. Neural networks can be used for such applications. When neural networks are designed specifically for pattern recognition, they perform essentially the role of signal processors, i.e., they extract the desired signal from unwanted noise. Many types of neural network algorithms have been employed in various applications related to signal processing [Ref 2]. In one particular application, a radar signal is processed using a backpropagation neural network filter for more effective detection of targets in a low signal to noise environment [Ref. 3]. Similarly, effective signal detection was achieved in a passive sonar system through the use of the backpropagation neural network [Ref 4]. The backpropagation neural network has also been used to enhance the performance of a continuous phase modulated receiver in satellite communications [Ref 5].

The backpropagation network is currently the most popular algorithm employed in filtering applications. The structure of the backpropagation network can be compared to that of a transversal filter with the exception of the hidden layers and nonlinear nature of the output function [Ref. 6:p.337]. In this study the backpropagation algorithm was used for filtering out the countermeasure noise from the telemetry signal.

B. BACKPROPAGATION THEORY

The basic building block of a backpropagation neural network is a perceptron which is also referred to as a processing element or node in the following. Figure 3.1 shows a model of the processing element used to form the backpropagation neural network.

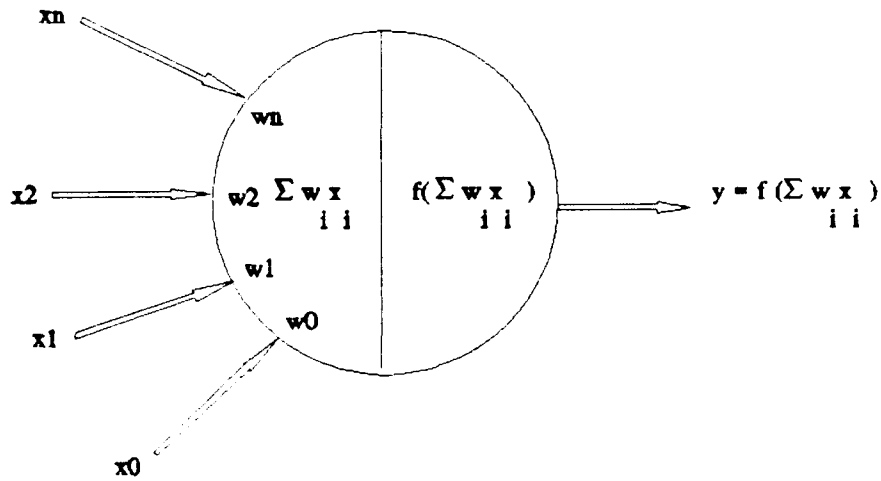


Figure 3.1 Perceptron Model.

In Figure 3.1, x_i are the input samples, w_i are the connection weights, and $f(\sum w_i x_i)$ is a nonlinear function. The operation of the processing element shown in Figure 3.1 can be mathematically stated as

$$y = f(\mathbf{w}^T \mathbf{x}) = f\left(\sum_{i=0}^n w_i x_i\right) \quad (3.1)$$

where

$$\begin{aligned} \mathbf{x} &= [x_0 \ x_1 \ x_2 \ \dots \ x_n]^T, \\ \mathbf{w} &= [w_0 \ w_1 \ w_2 \ \dots \ w_n]^T \end{aligned} \quad (3.2)$$

are $(n+1) \times 1$ vectors of input data and connection weights, respectively. In this implementation x_0 is always equal to 1 and is called the bias input [Ref. 3:p.57]. Typical nonlinear functions, shown in Figure 3.2, are the binary, sigmoid, threshold-

linear, and hyperbolic tangent [Ref. 7]. The hyperbolic tangent is used in this thesis because the inputs have both positive and negative values [Ref. 8].

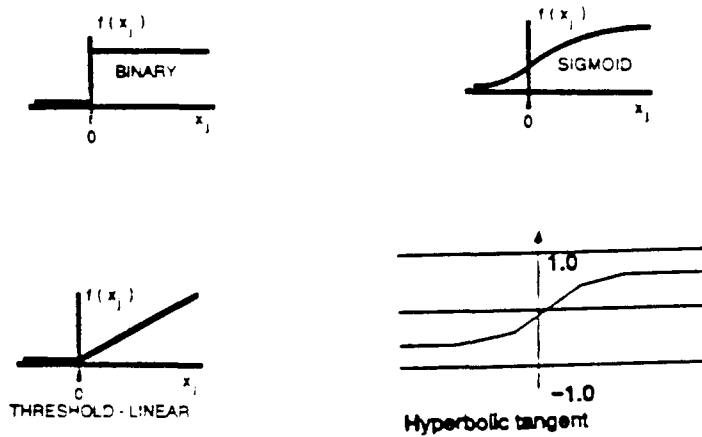


Figure 3.2 Examples of nonlinear functions used to modify the output of a given processing element.

A multilayer perceptron structure is obtained by arranging the basic elements of Figure 3.1 into multiple layers with each layer containing several basic elements. The backpropagation network is realized when Rosenblatt's back-propagated error correction method is used to update the connection weights [Ref. 7]. Figure 3.3 shows a typical backpropagation network. For clarity, only the connections from one node in a given layer to the next layer are shown. Backpropagation networks consist of an input layer, one or more hidden layers, and an output layer. Typically, a bias node is also included. In the input layer, each input node is connected to each first hidden layer node. The outputs of nodes in the first hidden layer are in turn provided as inputs to each node in the next layer. This process is repeated in each layer. Thus, Equation 3.1 may be rewritten as follows

$$x_{ij} = f(y_{ij}) = f\left(\sum_{i=0}^N w_{ji} x_{(i-1)i}\right) \quad (3.3)$$

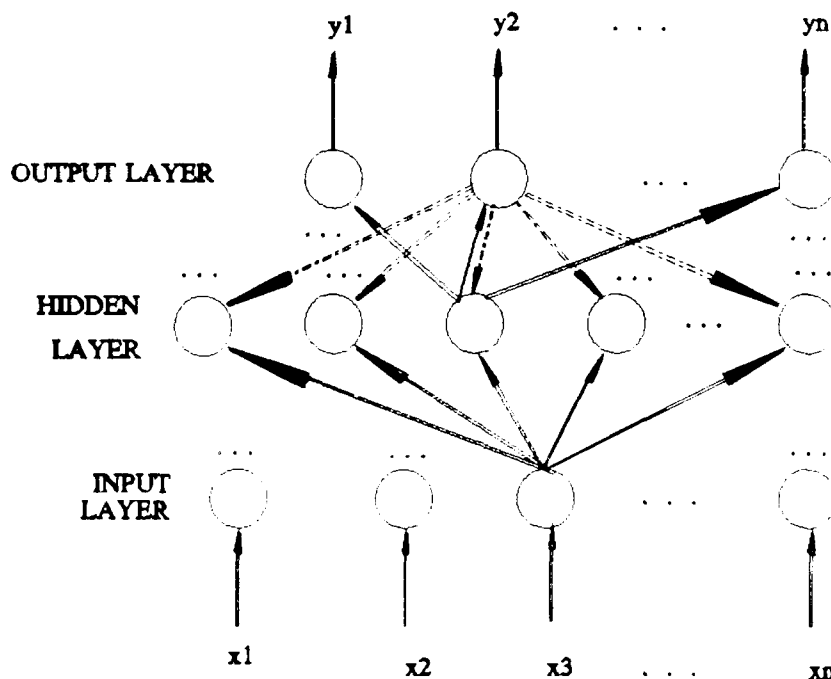


Figure 3.3 Backpropagation Network with input, output and one hidden layer.

where l is the layer number, j is the j^{th} element in the l^{th} layer, and i is the i^{th} element in $(l-1)^{\text{th}}$ layer. The last layer produces the output.

Two broad classes of backpropagation networks exist: the autoassociative network and the heteroassociative network. Both depend on the relation between the input vector x_i and the output vector y_i . When x_i equals y_i , the network is classified as an autoassociative network. This implies that both the input and output layer are of the same length. If the input and output layer are not the same length or if the elements in x_i do not equal the elements in y_i , then the network is classified as a heteroassociative network. [Ref. 6:p.80]

Typically, backpropagation networks are trained off-line by the supervised training technique. In supervised training, the network is supplied with a sequence

of correct input/output vector pairs $(x_1, y_1), (x_2, y_2), \dots (x_j, y_j)$. The output of the network is compared with the desired output, and the error between them is used to update the connection weights to correct and match the desired output [Ref. 6:p.48]. A more detailed description of how the error is corrected during supervised training follows.

The feedback lines, shown in Figure 3.3 as dashed lines, provide backpropagation of output errors to preceding layer nodes. These backpropagated error connections are used to update the weights of each node during training. The Widrow-Hoff learning law is used to update the weights here. The network is trained by randomly selecting one of the input vectors and processing the selected vector through the network. A comparison of the resulting network output with the desired output is then made. This error is used to adjust the connection weights in the feed forward path. Training is considered complete when the sum of squared errors or the cost function

$$J = 0.5 \sum_k (y_{desired_k} - y_{actual_k})^2, \quad (3.4)$$

where $y_{desired}$ is the desired output and y_{actual} is the actual output of the network, has been minimized. Since the cost function is a function of connection weights, the minimization is accomplished by adjusting the weight vector, \mathbf{w} , for each processing element in the layer.

Following the gradient descent technique used in the Widrow-Hoff learning law, the gradient of J is obtained as

$$\nabla_{\mathbf{w}} J(\mathbf{w}) = \left[\frac{\delta J}{\delta w_1}, \frac{\delta J}{\delta w_2}, \dots, \frac{\delta J}{\delta w_N} \right]^T. \quad (3.5)$$

For a k^{th} processing element in the l^{th} layer, the backpropagated error is given by where $f'(y_{actual})$ indicates the first derivative of $f(y_{actual})$. The connection weights are then updated according to

$$e_{lji} = - \frac{\delta J}{\delta w_{lji}} = - \frac{\delta J}{\delta y_{actual_{lji}}} \frac{\delta y_{actual_{lji}}}{\delta w_{lji}} \quad (3.6)$$

$$= - (y_{desired_{lji}} - y_{actual_{lji}}) f' (y_{actual_{lji}})$$

$$w_{lji}^{new} = w_{lji}^{old} - \alpha e_{lji} \quad (3.7)$$

where $\alpha > 0$ is called the learning coefficient [Ref. 6:p.136].

The manner in which the training data was presented to the backpropagation network in this research is a variation of that used by Khontanzad, Lu, and Srinath [Ref. 4]. Here the training data is divided into several sets. Each set contains the same cases of the desired signal. Differences between the sets is based on the amount of noise added to the signal. Training is accomplished in the following manner:

1. The network is first trained with the subset containing only examples of the ideal signal, i.e., with no noise added, until the mean-square error reaches a minimum.
2. The network is tested and results of the network performance are recorded.
3. Training is continued using the training data set containing the signal with noise added to the desired signal.
4. The network is tested again and the results of the network performance are recorded. The results are compared with the results from the previous testing cycle. If no improvement in the network performance has occurred, training is stopped.
5. If the network performance has improved, steps 3 and 4 are repeated with more noise added to the signal, i.e., at a lower SNR.

C. SOLUTION

Figure 3.4 shows a generalized solution model used in this research. Following preprocessing of the received signal, distinguishing features of the signal are extracted and input to the neural network. The neural network then processes this data to extract the tracking signal from the noise and provides a relatively noise free output for further processing.

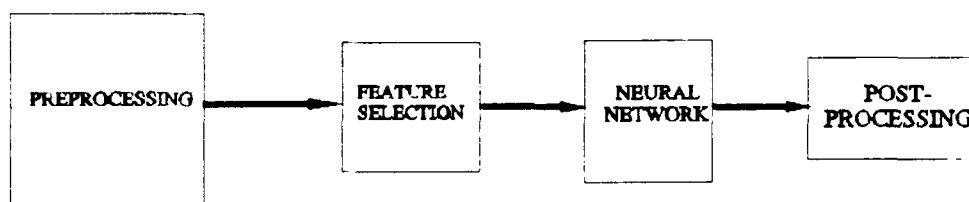


Figure 3.4 Schematic diagram of general solution model.

The features of the received signal used in this scheme in order to recover the tracking signal in noise are related to the power spectrum and are described in the next paragraph. An FFT algorithm is used for this purpose. The preprocessed data is sent to the FFT algorithm. The portion of the FFT samples containing the significant desired signal components of the BPSK spectral data is sent to the neural

network. The output from the network is postprocessed for further refinement and analysis.

Distinguishing transmitted binary sequences from their complement presents problems when detecting BPSK signals [Ref. 11]. The magnitude of the FFT is identical for two BPSK signals whose zeros and ones are reversed. Thus both the real and imaginary components of the FFT samples are used to overcome this ambiguity. Since the hydrophone attenuates information outside its frequency range, only a portion of the FFT samples covering the bandpass region around f_c with bandwidth equal to that of the tracking signal needs to be considered. For $f_c = 75$ kHz with a bandwidth of 20 kHz and a 84 point FFT, 12 samples centered about the carrier frequency are sufficient for this purpose. When the carrier frequency is removed by demodulation, the spectral content of the received signal is transformed to the baseband region. In this case the first 12 samples of the FFT are used as essential features of the signal.

The amount of preprocessing required is dependent on the location of the neural network within the receiver, i.e., bandpass or baseband. Preprocessing may consist of simply sampling the signal directly from the hydrophone as in the bandpass case. More complex preprocessing may be needed, with the incoming signal undergoing several alterations prior to being sent to the FFT algorithm as in the baseband case. Postprocessing depends on the required form of the output of the network, i.e., whether the network is used to produce a waveform of the tracking signal or to detect its bit sequence.

IV. SIMULATION RESULTS

A. INTRODUCTION

Due to the lack of analytical methods to evaluate the performance of networks, neural network performance is obtained through experimentation. Two general solutions are examined here, recovery of the desired BPSK signal for further processing and direct recovery of the binary code. The network's performance is examined in both the bandpass (with a carrier frequency of 75 kHz) and baseband regions. Performance of the network with different architectures, i.e., variations in the sizes of each of the hidden layers and output layer, is also evaluated. The Matlab package was used to implement both the pre- and postprocessing blocks of Figure 3.4 and the network is implemented using the Neuralware Professional Software Package [Ref. 8].

B. BANDPASS RESULTS

Two different neural network realizations are used to simulate the bandpass scheme. These are termed signal waveform recovery and binary code recovery. In the former, the desired output of the network is a relatively noise free BPSK signal. In the latter, the network output is the actual binary sequence. The architecture of the network used in each case is represented by the set of numbers $n_1-n_1-n_2-n_o$, where

n_1 is the number of input data samples, n_1 and n_2 represent the number of processing elements in the two hidden layers, and n_o is the number of output elements.

1. Signal Waveform Recovery

In this realization a 24-36-18-24 architecture is used for the network. This simulation examines the backpropagation algorithm's ability to filter the countermeasure noise from the received signal. Synchronization of the transmission time between the transmitter and the Nanoose range onshore processors is assumed to detect the start of the received noisy BPSK signal. Figure 4.1 shows a schematic diagram of this simulation. The received signal samples are placed in a buffer until 84 samples are collected. A 300 kHz sampling rate for $f_c = 75$ kHz is used which corresponds to 28 samples per bit. Thus, with an 84-point FFT, three bits worth of signal waveform is filtered simultaneously.

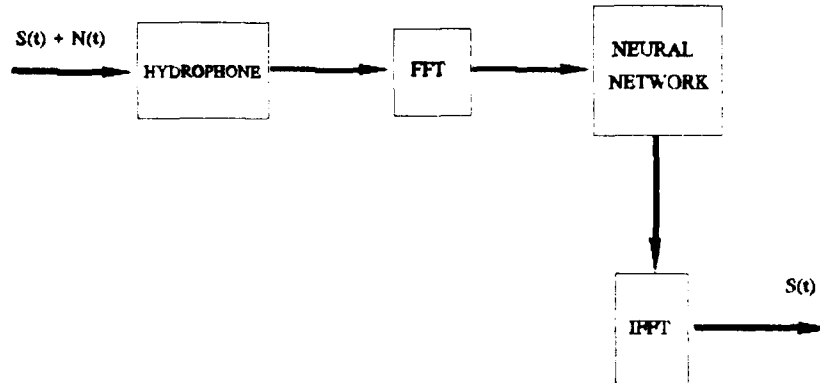


Figure 4.1 Model for direct signal recovery in the bandpass region.

Training was conducted in stages as detailed in section B of Chapter III. The training data set contained all of the possible combinations representing the binary code for three bits with the SNRs of ∞ dB (no noise), 5 dB, 0 dB, and -5 dB. Since the noise is white, three training examples using different random sequences of the noise are used. During each stage only the direct path noise from the countermeasure to the hydrophone is considered.

Figure 4.2 shows an example of the filtering performed by this neural network. The signal represents a binary code of 1 0 0 with countermeasure noise added at an SNR of 0 dB. Figure 4.2a shows the signal received by the hydrophone. Figure 4.2b shows the signal received at the output of the hydrophone. Finally, Figure 4.2c shows the inverse FFT of the signal after it has been processed by the neural network. This signal is presented for decoding.

The results of testing showed that the neural net could recover the signal at SNRs down to 0 dB. At SNRs lower than 0 dB, this network was not able to extract the BPSK signal accurately. A method for direct recovery of the binary code is examined next.

2. Binary Code Recovery

In the foregoing method, further processing is required to obtain the output in the binary form. Figure 4.3 shows the block diagram of the binary code recovery scheme. The neural network is configured as shown in Table 4.1. Note the differences in the number of nodes in each layer.

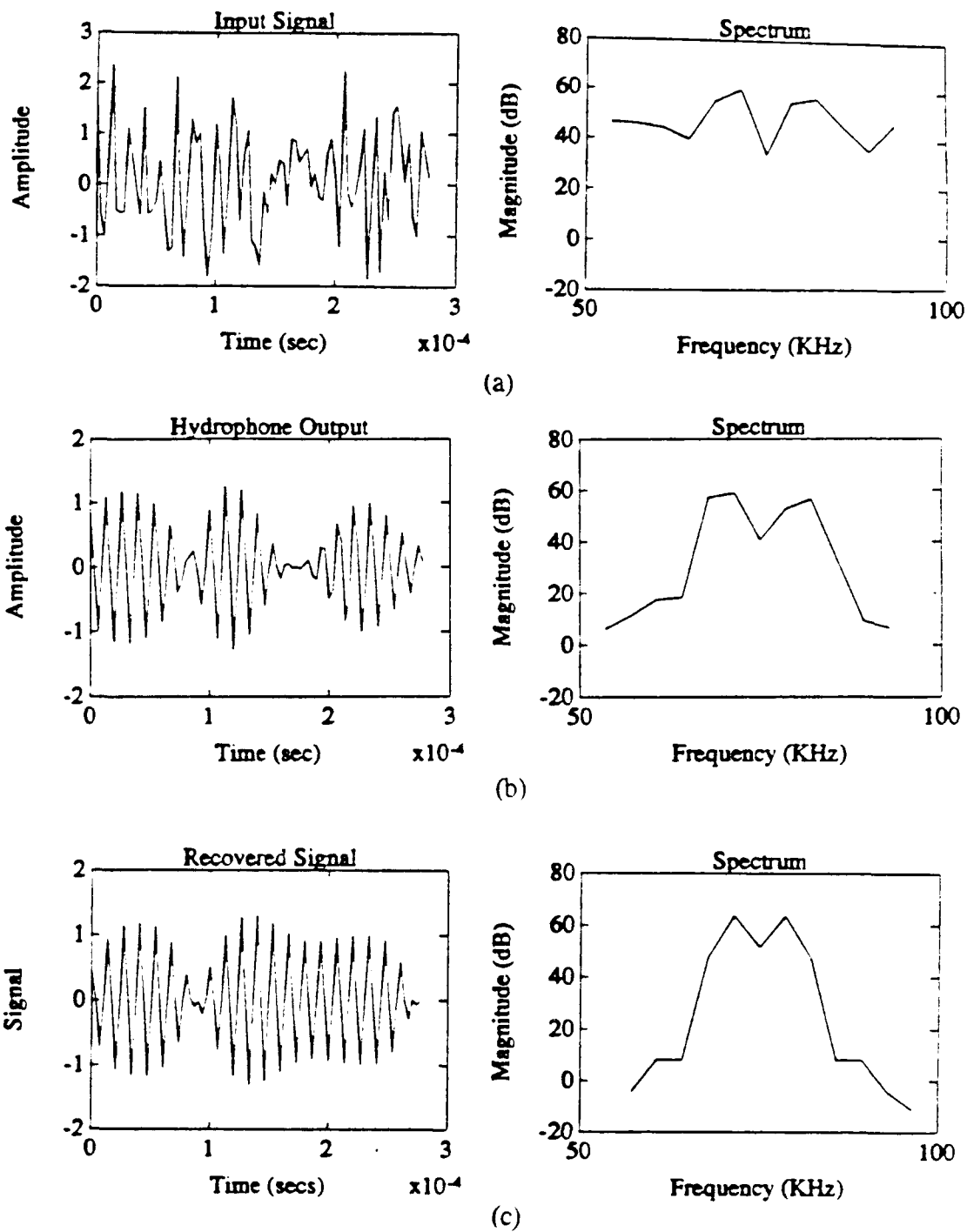


Figure 4.2 (a) Signal input to the hydrophone and power spectrum. (b) Signal input to FFT and power spectrum. (c) Processed signal output and power spectrum.

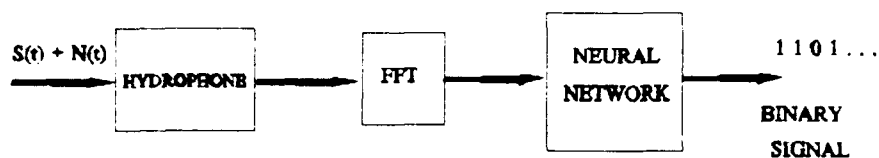


Figure 4.3 Model for direct code recovery in the bandpass region.

TABLE 4.1

Number of Recovered Bits	Number of Nodes per Layer
2	24-16-8-2
3	24-18-9-3
4	24-18-12-4

A series of four Monte Carlo simulations were conducted on each of the three neural network configurations to test direct recovery of binary code. The four simulations examined the network's performance in the following areas: direct path noise only, multipath noise, variations in the network architecture, and consistent doppler effects. In each simulation a fixed 48 bit code was used and the SNR level was varied every 5 dB, from 10 to -20. At each SNR 100 different noise realizations

were used to carry out a Monte Carlo simulation. Although three networks were evaluated with the Monte Carlo simulation, results of a single network, the 4 bit recovery network, are detailed below.

The first Monte Carlo simulation examined the network performance after successive stages of training at ∞ dB, 5 dB, 0 dB, and -5 dB SNRs was completed. The noise model used was the direct path model. Figure 4.4 shows the neural network performance after each stage of training has been completed. After each stage the network performance improved. This improvement is attributed to continuously training the neural network to noisy examples of the signal. When trained with a data set at a SNR of -10 dB, however, the performance became worse. (For the 2 and 3 bit cases this degradation occurred at -5 dB.)

The second Monte Carlo simulation examined the network, trained in the first simulation, when the countermeasure noise arrived from both direct path and surface reflection. Figure 4.5 shows the results with the network trained to -5 dB. The results from the first simulation after the network was trained are also shown for comparison. Performance for each case is almost identical.

The third test was an entire series of Monte Carlo simulations. These simulations studied the performance trends when the hidden layers are altered in size. These results, which are presented in Table 4.2 below, represent the estimated probability of bit error for the 48-bit binary code sequence.

Holding the number of nodes in the second hidden layer constant and increasing the number of nodes in hidden layer one, degraded the performance of

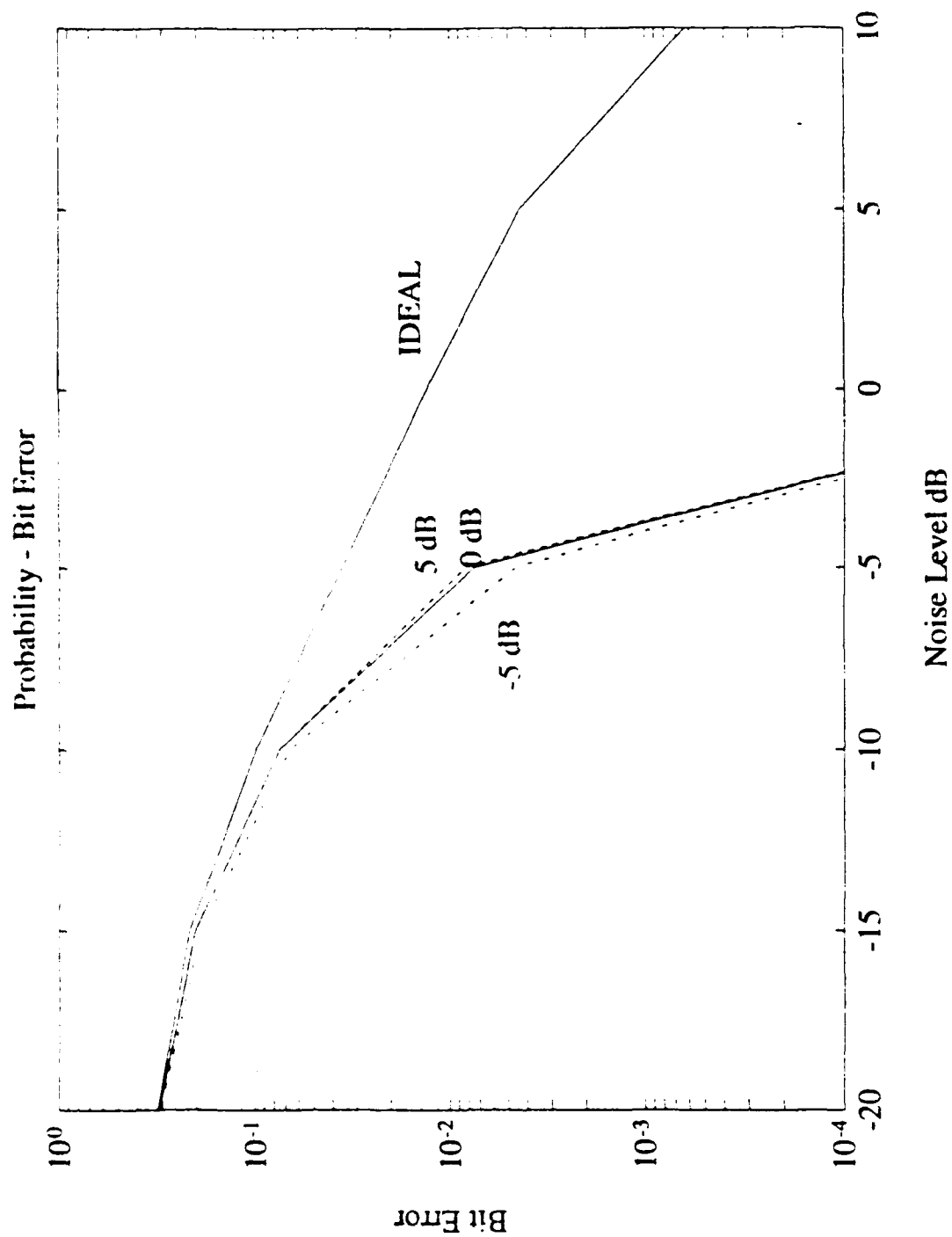


Figure 4.4 Network performance after each training stage for the Four Bit Direct Recovery Network.

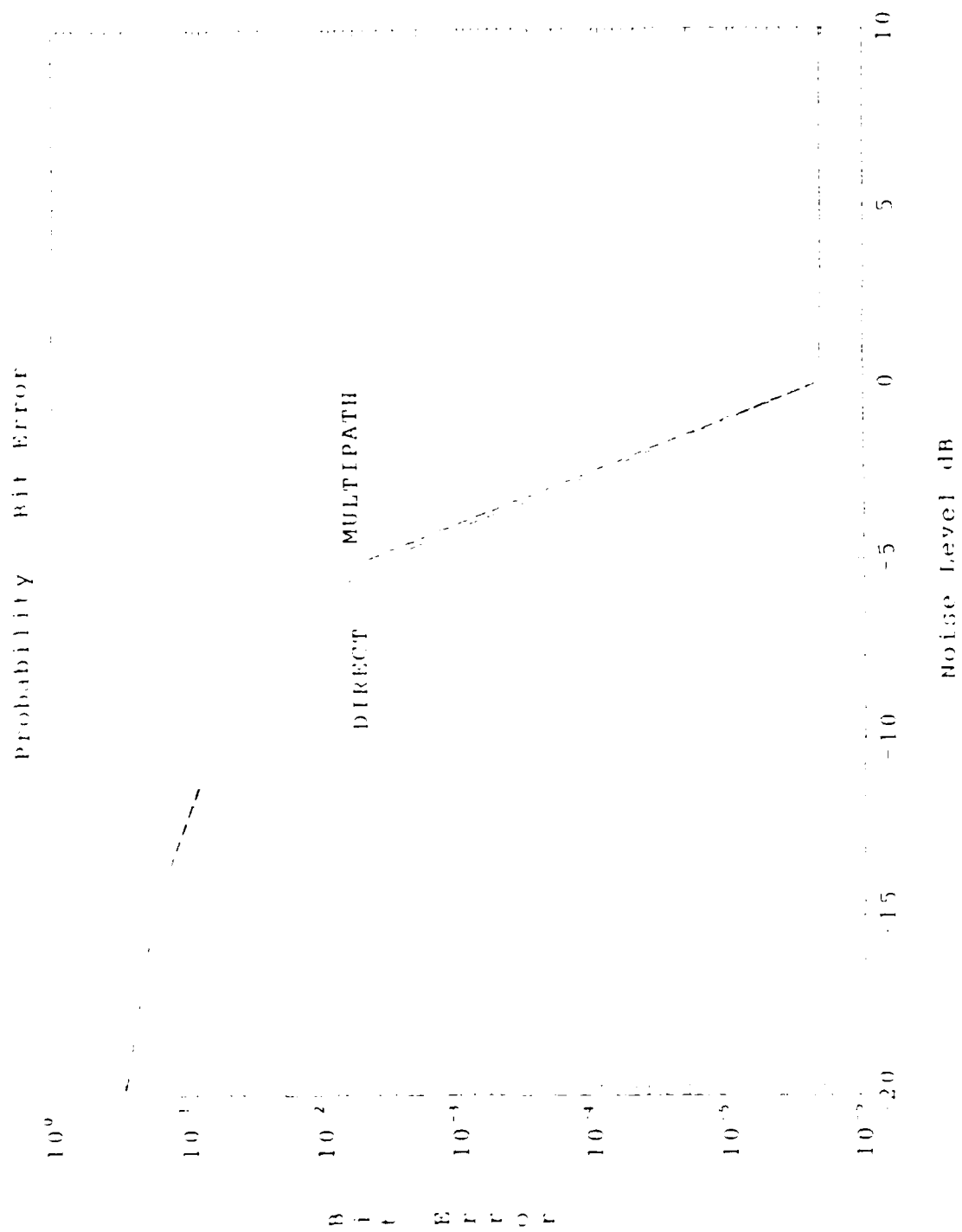


Figure 4.5 Multipath vs. Direct path propagation of Countermeasure noise.

TABLE 4.2

HL-1	HL-2	-5 dB	-10 dB	-15 dB	-20 dB
24	16	0.0025	0.064	0.185	0.307
24	12	0.0065	0.076	0.204	0.315
24	8	0.0033	0.064	0.185	0.305
18	16	0.0035	0.062	0.190	0.307
18	12	0.0048	0.066	0.190	0.302
18	8	0.0038	0.065	0.190	0.308
12	16	0.0031	0.065	0.192	0.305
12	12	0.0031	0.064	0.185	0.302
12	8	0.0065	0.076	0.208	0.318

the network. With the number of nodes in the first layer constant, increasing the number of in the second layer from the original 12 nodes improved the performance of the network.

The fourth Monte Carlo simulation in the bandpass region concerned the effect of doppler shift on the neural network's performance. The network failed this simulation. To help determine the cause of this failure, a carrier phase offset was added to the signal model. Figure 4.6 shows the results of this simulation for various phase offsets. Note that as the phase offset increases the performance of the network degrades.

The direct binary code recovery scheme produced much better results than the signal recovery method, discussed earlier. The presence of multipath countermeasure noise did not severely affect the performance of the network. The

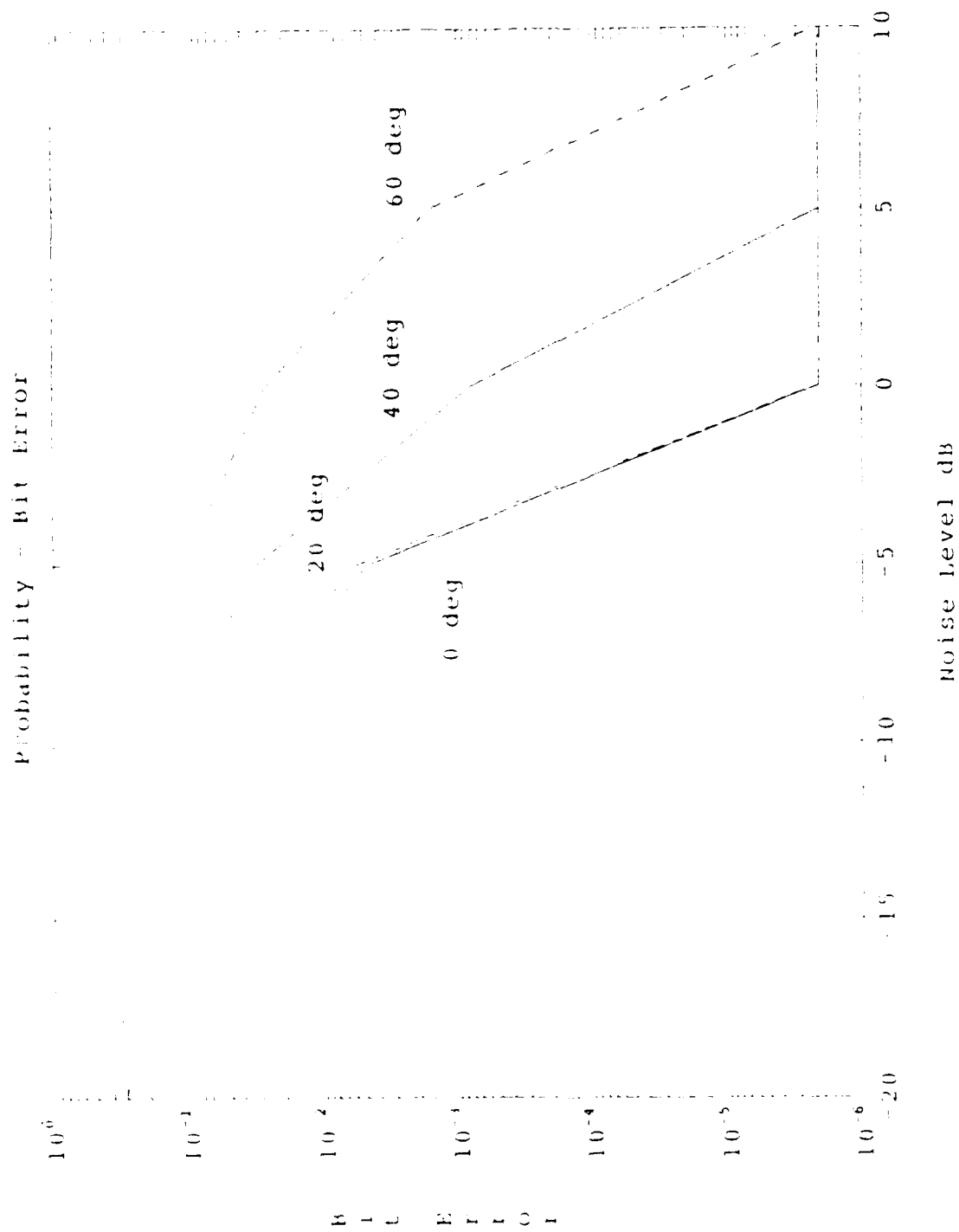


Figure 4.6 Monte Carlo simulations with various phase delays.

major disadvantage is the sensitivity of the network to changes in phase. Doppler shifts of the signal alter both frequency and phase of the spectral information degrading recovery of the signal.

C. BASEBAND RESULTS

Figure 4.7 shows the block diagram for the baseband scheme for direct recovery of binary code. The lowpass filter is required to eliminate the unwanted high frequency components after the received signal is multiplied by the local reference carrier. The input to the neural network now consists of the first 12 complex samples of the FFT. Only the results from Monte Carlo simulations corresponding to the first and fourth Monte Carlo simulations of the bandpass case discussed in section B are presented. Performance of the three networks were once again consistent with each other, therefore only the 4 bit recovery results are presented here.

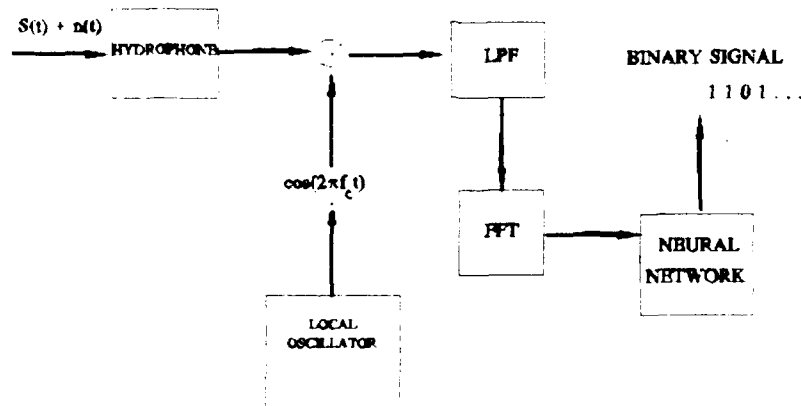


Figure 4.7 Model for direct code recovery in the baseband region.

The first baseband Monte Carlo simulation tested the performance of the baseband 4-bit neural network after each stage of training. Figure 4.8 shows the Monte Carlo response after each stage of training. Once again the introduction of noisy signal examples helped to train the neural network more effectively.

The fourth baseband Monte Carlo simulation examined the effect of doppler on the 4-bit recovery network. This simulation used the trained neural network from the first simulation and two Monte Carlo simulations were conducted using two different sampling rates. In both simulations a phase lock loop was assumed incorporated as part of the demodulating scheme to determine the local oscillator frequency. It was assumed that the phase lock loop was locked on to the signal providing accurate demodulation of the signal. Sampling was conducted at a constant 300 kHz for one simulation and was varied to maintain a four times oversampling in the second data set. Figure 4.9 shows the results for the constant sampling rate at 300 kHz. Note that the network handled the doppler effects, but the increase in the doppler shift resulted in increased bit errors.

Figure 4.10 shows the results with a constant sampling rate of four times the frequency of the local oscillator controlled by the phase locked loop. The advantage of using a coherent detection scheme to directly recover the code is that doppler effects are minimized. Additionally all the advantages of direct code recovery still apply when in the bandpass region. The disadvantages are that the phase lock loop must be able to capture and lock on to the incoming signal carrier frequency in spite of the noise, otherwise the signal can not be recovered accurately. The second

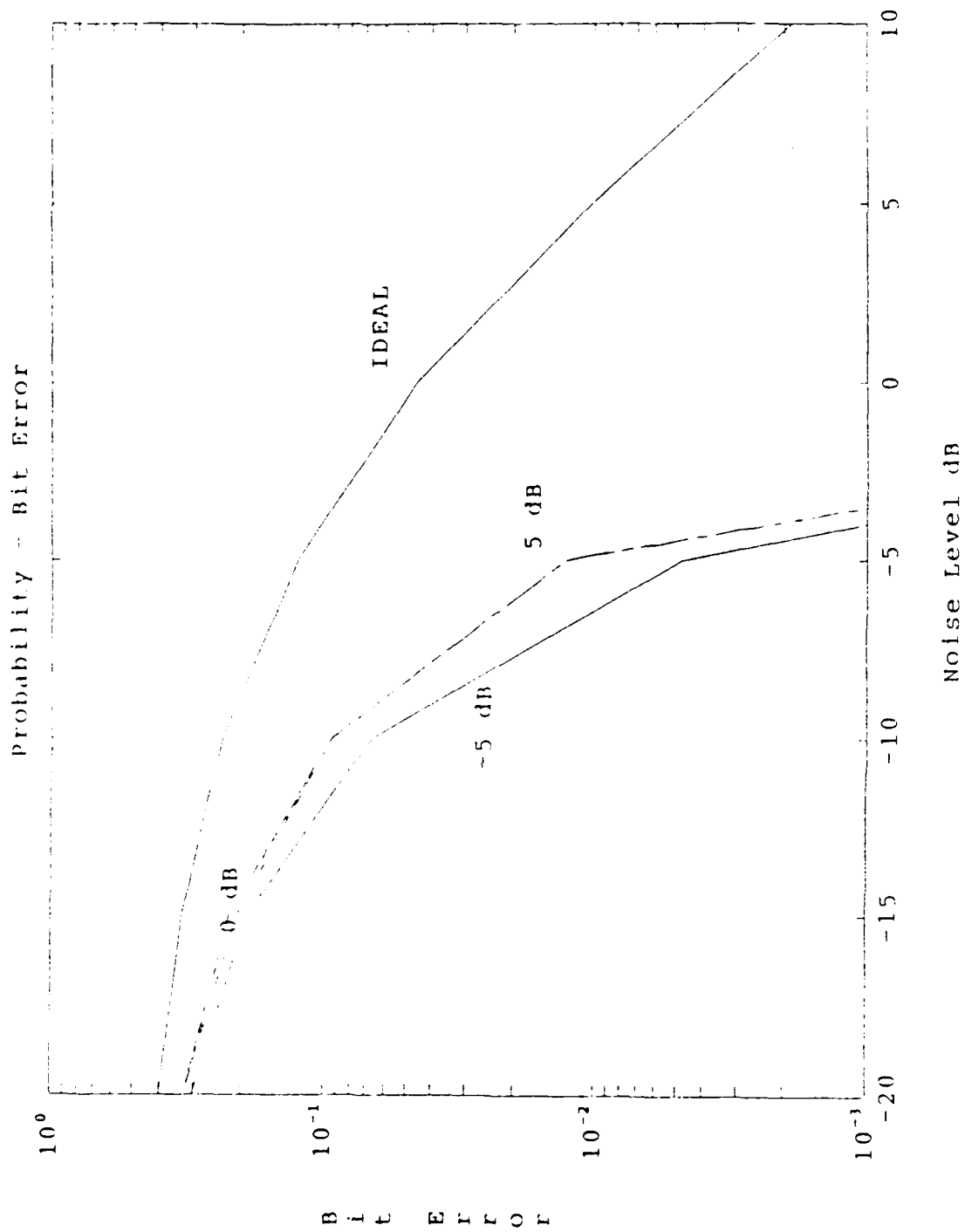


Figure 4.8 Network performance after each training stage for the Four Bit Direct Recovery Network in the baseband region.

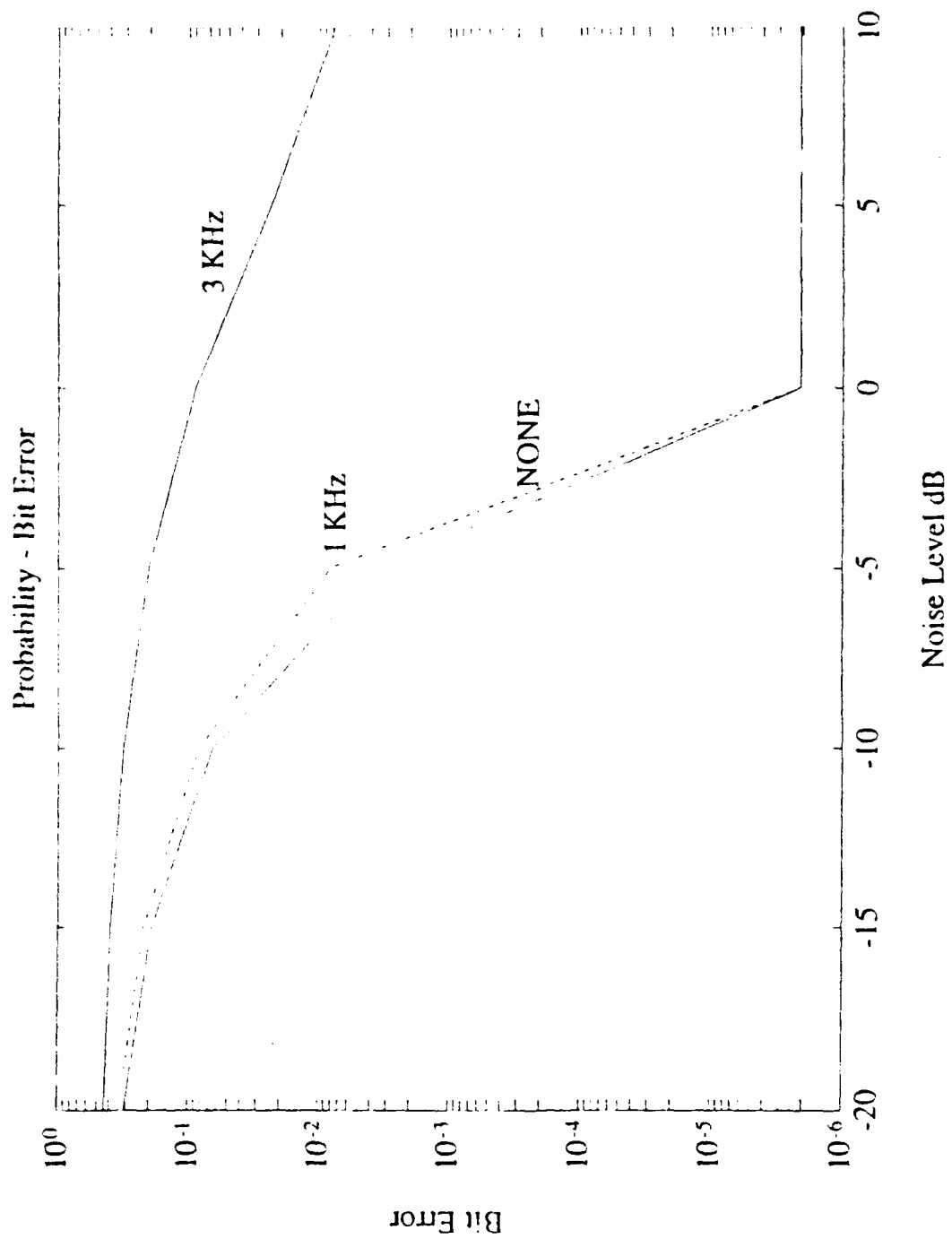


Figure 4.9 Doppler effects with sampling rate held constant.

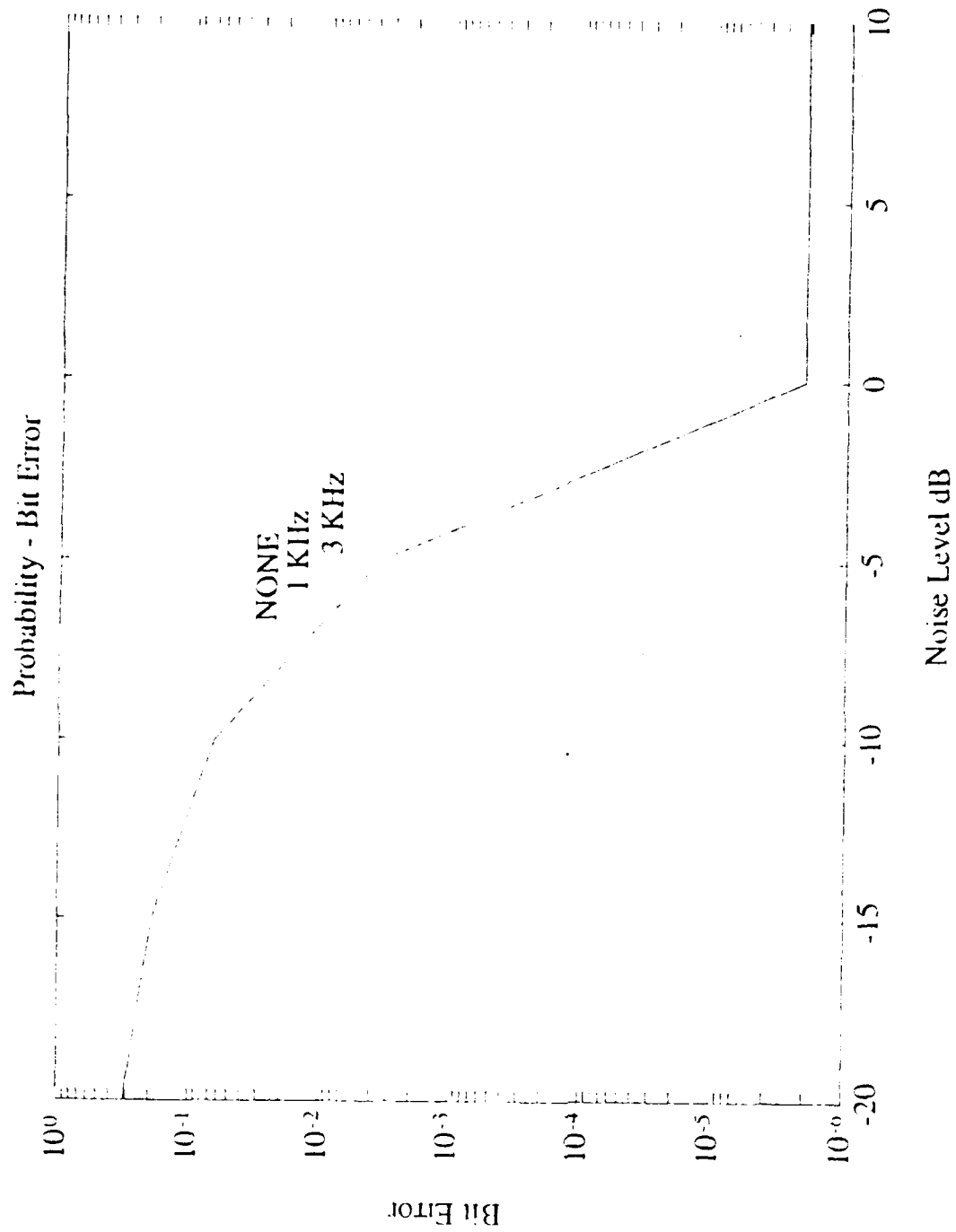


Figure 4.10 Doppler effects for constant four time oversampling rate.

disadvantage is that to eliminate the doppler effects a variable sampling frequency must be employed. While easy to do in a computer simulation, physically this is not easily implemented.

V. CONCLUSIONS AND RECOMMENDATIONS

A. CONCLUSIONS

The problem addressed in this thesis was to recover torpedo telemetry data masked by an acoustic broadband countermeasure. Several neural networks employing the backpropagation algorithm were examined for this purpose. Of those examined the recommended network is the four bit direct code recovery network, developed for the baseband region.

Several simulation results were obtained. The most important result is that direct code recovery is feasible using spectral feature information. Successful recovery of the binary code is possible with SNRs of approximately -10 dB or higher. For lower SNRs (< -10 dB) the performance falls off rapidly. Additionally, the neural network performance is nearly the same for direct path and multi-path noise environments considered in this work.

The largest problem encountered with this approach is the phase sensitivity of the neural network. Demodulating the signal to the baseband region will decrease this sensitivity, but a phase locked loop is required for accurate demodulation. To completely eliminate the phase sensitivity caused by doppler effects, a variable sampling rate scheme is proposed.

B. RECOMMENDATIONS

This research examined only one possible input feature selection of the signal. Other feature selections should be examined. One such feature selection could be the autocorrelation of the signal.

The acoustic environment model used is a simplistic model. In an actual implementation, the acoustic environment constantly changes, thus making off-line training less practical. Since the object identity code part of the bit sequence is known a priori, this sequence could be exploited to train the network on-line to adapt to the existing acoustic conditions.

APPENDIX A.

```

function[xn,t,bits]=wavecode(code,c)
% [xn,t] = wavecode(code,c)
%
% This program generates a waveform for sampling.
%
%      xn = the generated waveform
%      t  = the time index
%      code = the six digit binary code sequence
%            ie. [1 0 1 1 0 0]
%      f   = the freq of the wave
%      fs  = the sampling freq
%      cd  = the code expanded into each sample
%      bits = the bit numbers for the x axis
%      c   = the number of bits in the code

f=75000;                %freq of the waveform

s=4;                    %samples per cycle
fs=s*f;                %sampling rate
cpb=7;                  %number of cycles per bit
b=3;                    %number of blocks of code
T=cpb/f;                %time for one bit

t=0:c*cpb*b*s-1;        % number of samples
t=t/fs;                 % the sample times
bits=1:c*cpb*b*s;
bits=(bits./(s*cpb))+1; % the bits index

% build up the code to the samples per bit

for n =1:length(code)
    for m=1:s*cpb        % s*cpb is the samples per bit
        cd=[cd code(n)]; % This expands the code so each code digit is
    end                 % the same for the length of a bit
end
a=[];

for x=1:b                % build the code for the entire sequence
    a=[a cd];            % where b is the number of blocks of data
end

for n=1:length(a)
    if a(n)==0
        a(n)=-1;
    end
end

xn=a .* cos(2*pi*f*t);    % the waveform

```

```
% Datagen84.m generates training sets to train a neural network
%to recover the FFT components of BPSK signal, filtering unwanted
%noise components. The signal waveform for three bits of the binary
%code is used for the FFT.
```

```
numbin=84;
load code3bit;
wn=[65e3 85e3]/((75e3*4)/2);
[b,a]=butter(6,wn);
temp1=49;
temp2=132;
rand('normal');
rand('seed',5);
for l=1:4
dB=5;
for k=1:32
Noiseamp=(1/sqrt(2))*10^(-dB/20);
[ideal_signal,time]=wavecode(code3bit(k,:),5);
Noise=rand(time);
signal=ideal_signal+Noiseamp*Noise;
filtered_signal=filter(b,a,signal);
ideal_fil_signal=filter(b,a,ideal_signal);
y2=fft(filtered_signal(temp1:temp2),numbin);
y3=fft(signal(temp1:temp2),numbin);
data=[0 0;0 0];
y4=[y2;y3];
for j=1:12
data=[data real(y4(:,(j+16))) imag(y4(:,(j+16)))];
end;
if k == 1,
magdat=[data(:,3:26)];
else
magdat=[magdat;data(:,3:26)] ;
end;
end;
if l==1
training_data=magdat;
else
training_data=[training_data; magdat];
end;
end;
[R C]=size(training_data);
for n=1:R
for k=1:C
if abs(training_data(n,k))<1e-4
training_data(n,k)=0.0;
end;
end;
end;
end;
save bpdats.nna training_data /ascii;
```



```
% Datagenbitcomp.m generates the training sets used in training
%neural networks to recover a BPSK signal in noise. To obtain the
%ideal BPSK signal the FFT of the ideal signal is used. To obtain
%data sets of the ideal BPSK signal with noise the variable signal
% or lpfsignal are used. The SNR level is controlled by setting
%the dB level. The portion of the FFT containing the BPSK spectral
%information is placed in a file with the corresponding binary code
%sequence to train the neural network.
```

```
numbin=112;
load code2bit.mat;           %Load binary code training sets
load code3bit.mat;
load code4bit.mat;
wn=[65e3 85e3]/((75e3*4)/2); %Hydrophone model
[b,a]=butter(6,wn);
bb=fir1(40,10e3/150e3);      %Low pass filter
temp1=41;
temp2=124;
rand('normal');
rand('seed',20);
for l=1:4
    dB=5;                    %Set SNR level
    for k=1:64               %Loop for 4 bit code generation.
        Noiseamp=(1/sqrt(2))*10^(-dB/20);
        [ideal_signal,time]=wavecode(code4bit(k,:),6);
        Noise=rand(time);
        signal=ideal_signal+Noiseamp*Noise;
        filtered_signal=filter(b,a,signal);
        ideal_fil_signal=filter(b,a,ideal_signal);
        mod_signal=filtered_signal.*cos(150e3*pi*time);
        lpf_signal=filter(bb,1,mod_signal);
        y2=fft(filtered_signal( 49:160),numbin);
        y3=fft(lpf_signal(69:180),numbin);
        data2=[0 0];
        data3=[0 0];
        for j=1:12
            data2=[data2 real(y2(:,(j+23))) imag(y2(:,(j+23)))];
            data3=[data3 real(y3(:,(j+0))) imag(y3(:,(j+0)))];
        end;

        if k == 1
            magdat2=[data2(:,3:26) code4bit(k,2:5)];
            magdat3=[data3(:,3:26) code4bit(k,2:5)];
        else
            magdat2=[magdat2;data2(:,3:26) code4bit(k,2:5)];
            magdat3=[magdat3;data3(:,3:26) code4bit(k,2:5)];
        end;
    end;

    if l==1
        training_data2=magdat2;
        training_data3=magdat3;
    else
        training_data2=[training_data2; magdat2];
        training_data3=[training_data3; magdat3];
    end;
end;
[R C]=size(training_data2);
for n=1:R
    for k=1:C
```

```

end;
end;
[R C]=size(training_data5);
for n=1:R
for k=1:C
    if abs(training_data5(n,k))<1e-4
        training_data5(n,k)=0.0;
    end;
end;
end;
end;
save bittrdat3.nna training_data4 /ascii;
save bb3bittrdat.nna training_data5 /ascii;

numbin=56;
rand('seed',20);
for l=1:4
dB=5;                                     %Loop for 2 bit code generation
for k=1:16
Noiseamp=(1/sqrt(2))*10^(-dB/20);
[ideal_signal,time]=wavecode(code2bit(k,:),4);
Noise=rand(time);
signal=ideal_signal+Noiseamp*Noise;
filtered_signal=filter(b,a,signal);
ideal_fil_signal=filter(b,a,ideal_signal);
mod_signal=filtered_signal.*cos(150e3*pi*time);
lpf_signal=filter(bb,1,mod_signal);
y6=fft(ideal_fil_signal(49:104),numbin);
y7=fft(lpf_signal(69:124),numbin);
data6=[0 0];
data7=[0 0];
for j=1:12
data6=[data6 real(y6(:,(j+8))) imag(y6(:,(j+8))))];
data7=[data7 real(y7(:,(j+0))) imag(y7(:,(j+0))))];
end;
if k == 1
magdat6=[data6(:,3:26) code2bit(k,2:3)];
magdat7=[data7(:,3:26) code2bit(k,2:3)];
else
magdat6=[magdat6;data6(:,3:26) code2bit(k,2:3)];
magdat7=[magdat7;data7(:,3:26) code2bit(k,2:3)];
end;
end;
if l==1
training_data6=magdat6;
training_data7=magdat7;
else
training_data6=[training_data6; magdat6];
training_data7=[training_data7; magdat7];
end;
end;
[R C]=size(training_data7);
for n=1:R
for k=1:C
    if abs(training_data7(n,k))<1e-4
        training_data7(n,k)=0.0;
    end;
end;
end;
end;
[R C]=size(training_data7);
for n=1:R

```

```
for k=1:C
    if abs(training_data7(n,k))<1e-4
        training_data7(n,k)=0.0;
    end;
end;
end;
end;
save bittrdat2.nna training_data6 /ascii;
save bb2bittrdat.nna training_data7 /ascii
```

```

function[xn,t]=montewavecode(code)
% [xn,t] = wavecode(code)
%
% This program generates a waveform for sampling.
%
%      xn = the generated waveform
%      t = the time index
%      code = the six digit binary code sequence
%             ie. [1 0 1 1 0 0]
%      f = the freq of the wave
%      fs = the sampling freq
%      cd = the code expanded into each sample
%      bits = the bit numbers for the x axis

f=75000;           %freq of the waveform
s=4;               %samples per cycle
fs=s*f;           %sampling rate
c=48;              %number of bits in the code
cpb=7;             %number of cycles per bit
b=1;               %number of blocks of code
T=cpb/f;          %time for one bit

t=0:c*cpb*b*s-1;  % number of samples
t=t/fs;           % the sample times
bits=1:c*cpb*b*s;
bits=(bits./(s*cpb))+1; % the bits index

% build up the code to the samples per bit

for n =1:length(code)
    for m=1:s*cpb
        cd=[cd code(n)];
    end
end
a=[];

for x=1:b
    a=[a cd];
end

for n=1:length(a)
    if a(n)==0
        a(n)=-1;
    end
end

xn=a .* cos(2*pi*f*t); % the waveform

```

```

% This program generates test data for Monte Carlo simulations.
%Data sets for recovering 2, 3, and 4 bits are generated. Direct path
%and multi-path noise models may be used. The undesired model must
%be commented out (%). For schemes involving the bandpass region
%the FFT of hydrosignal is used and for the baseband region lpfsignal
%is used.
%
%
load montecode;           % Loads a 48 bit binary code of 1 & 0 from a
dB=-20:5:10;              %file called montecode.
[dessignal,time]=montewavencode(montecode); %Generates BPSK signal.
rand('normal');
wn=[65e3 85e3]/150e3;     % Hydrophone Model
[b,a]=butter(6,wn);
bb=fir1(40,10e3/150e3); % Low Pass Filter
for k=1:7
dB(k)
NoiseAmp=(1/sqrt(2))*10^(-dB(k)/20);
for m=1:25
    rand('seed',m);
    temp1=41;
    temp2=96;
    Noise=rand(time); %White noise; direct path.
    signal= dessignal + NoiseAmp*Noise;
    %Noise=NoiseAmp*rand([time time]); %White noise; multi-path.
    [r,c]=size([time time]);
    %A=0.9;
    %B=sqrt(1-(A^2));
    %DirectNoise=A*Noise(1:c/2);
    %ReflectedNoise=B*Noise((c/2)+1:c);
    %signal=dessignal + DirectNoise + ReflectedNoise;
    hydrosignal=filter(b,a,signal); %Bandpass region
    modsignal=hydrosignal.*cos(2*78e3*pi*time); %Demodulator
    lpfsignal=filter(bb,1,modsignal); %Baseband region

    for j=1:24 %Two Bit
        y=fft(lpfsignal(temp1:temp2),56);
        data=[0 0];
        for n=1:12
            data=[data real(y(n+0)) imag(y(n+0))];
        end;
        if j==1 & k==1 & m ==1
            twobit=data(3:26);
        else
            twobit=[twobit; data(3:26)];
        end;
        temp1=temp2+1;
        temp2=temp1+55;
    end;
    temp1=41;
    temp2=124;
    for j=1:16 %3 Bit
        y=fft(lpfsignal(temp1:temp2),84);
        data=[0 0];
        for n=1:12
            data=[data real(y(n+0)) imag(y(n+0))];
        end;
        if j==1 & k==1 & m ==1
            threebit=data(3:26);
        else
            threebit=[threebit; data(3:26)];
        end;
    end;
end;

```

```

        threebit=[threebit;data(3:26)];
    end;
    temp1=temp2+1;
    temp2=temp1+83;
end;
temp1=41;
temp2=152;
for j=1:12                                %4 Bit
    y=fft(lpfsignal(temp1:temp2),112);
    data=[0 0];
    for n=1:12
        data=[data real(y(n+0)) imag(y(n+0))];
    end;
    if j==1 & k==1 & m==1
        fourbit=data(3:26);
    else
        fourbit=[fourbit;data(3:26)];
    end;
    temp1=temp2+1;
    temp2=temp1+111;
end;

end;

end;

save bmtst2.nna twobit /ascii;
save bmtst3.nna threebit /ascii;
save bmtst4.nna fourbit /ascii;

```

APPENDIX B.

Title: Baseband 4 Bit Recover Code Network

Display Mode: Network

Display Style: baseband4bit

Control Strategy: backprop

Type: Hetero-Associative

36000 Learn

0 Recall

L/R Schedule: backprop

0 Layer

64 Aux 1

0 Aux 2

0 Aux 3

L/R Schedule: backprop

Recall Step	1	0	0	0	0
Input Clamp	0.0000	0.0000	0.0000	0.0000	0.0000
Firing Density	100.0000	0.0000	0.0000	0.0000	0.0000
Temperature	0.0000	0.0000	0.0000	0.0000	0.0000
Gain	1.0000	0.0000	0.0000	0.0000	0.0000
Gain	1.0000	0.0000	0.0000	0.0000	0.0000
Learn Step	5000	0	0	0	0
Coefficient 1	0.9000	0.0000	0.0000	0.0000	0.0000
Coefficient 2	0.6000	0.0000	0.0000	0.0000	0.0000
Coefficient 3	0.0000	0.0000	0.0000	0.0000	0.0000
Temperature	0.0000	0.0000	0.0000	0.0000	0.0000

IO Parameters

Learn Data: File Rand. (bbfourbittrdatn5) Load

Recall Data: File Seq. (bmtst4)

Result File: Desired Output, Output

UserIO Program: userio

I/P Ranges: -1.0000, 1.0000

O/P Ranges: -0.0000, 1.0000

I/P Start Col: 1

O/P Start Col: 25

MinMax Table: bb4bit

Number of Entries: 28

MinMax Table <bb4bit>:

Col:	1	2	3	4	5	6
Min:	-73.6726	0.0000	-41.7620	-50.3426	-17.1389	-36.9299
Max:	81.33	0	43.71	47.82	18.32	45.52
Col:	7	8	9	10	11	12
Min:	-15.9573	-18.1307	-7.6273	-8.7769	-2.6629	-4.9957
Max:	15.97	18.1	6.603	8.388	3.26	5.771
Col:	13	14	15	16	17	18
Min:	-1.5988	-3.7417	-1.1476	-3.1468	-0.9116	-2.7222
Max:	1.71	4.394	1.226	3.69	0.9681	3.176
Col:	19	20	21	22	23	24
Min:	-0.8300	-2.4128	-0.7747	-2.1625	-0.7351	-1.9560
Max:	0.8542	2.791	0.8089	2.501	0.7762	2.264
Col:	25	26	27	28		
Min:	0.0000	0.0000	0.0000	0.0000		
Max:	1	1	1	1		

Layer: 1

PEs: 1

Wgt Fields: 2

Sum: Sum

Spacing: 5

F' offset: 0.00

Transfer: Linear

Shape: Square

Output: Direct

Scale: 1.00

Low Limit: -9999.00

Error Func: standard

Offset: 0.00

High Limit: 9999.00

Learn: --None--

Init Low: -0.100

Init High: 0.100

L/R Schedule: (Network)

Winner 1: None

Winner 2: None

PE: Bias

1.000 Err Factor

0.000 Desired

0.000 Sum

1.000 Transfer

1.000 Output

0 Weights

-55.901 Error

0.000 Current Error

Layer: In

PEs: 24	Wgt Fields: 1	Sum: Sum
Spacing: 5	F' offset: 0.00	Transfer: Linear
Shape: Square		Output: Direct
Scale: 1.00	Low Limit: -9999.00	Error Func: standard
Offset: 0.00	High Limit: 9999.00	Learn: --None--
Init Low: -0.100	Init High: 0.100	L/R Schedule: (Network)
Winner 1: None		Winner 2: None

PE: 2	1.000 Err Factor	0.097 Desired	
	0.097 Sum	0.097 Transfer	0.097 Output
	0 Weights	0.000 Error	0.000 Current Error
PE: 3	1.000 Err Factor	0.000 Desired	
	0.000 Sum	0.000 Transfer	0.000 Output
	0 Weights	0.000 Error	0.000 Current Error
PE: 4	1.000 Err Factor	0.164 Desired	
	0.164 Sum	0.164 Transfer	0.164 Output
	0 Weights	0.000 Error	0.000 Current Error
PE: 5	1.000 Err Factor	-0.120 Desired	
	-0.120 Sum	-0.120 Transfer	-0.120 Output
	0 Weights	0.000 Error	0.000 Current Error
PE: 6	1.000 Err Factor	-0.261 Desired	
	-0.261 Sum	-0.261 Transfer	-0.261 Output
	0 Weights	0.000 Error	0.000 Current Error
PE: 7	1.000 Err Factor	0.047 Desired	
	0.047 Sum	0.047 Transfer	0.047 Output
	0 Weights	0.000 Error	0.000 Current Error
PE: 8	1.000 Err Factor	-0.161 Desired	
	-0.161 Sum	-0.161 Transfer	-0.161 Output
	0 Weights	0.000 Error	0.000 Current Error
PE: 9	1.000 Err Factor	0.005 Desired	
	0.005 Sum	0.005 Transfer	0.005 Output
	0 Weights	0.000 Error	0.000 Current Error
PE: 10	1.000 Err Factor	-0.067 Desired	
	-0.067 Sum	-0.067 Transfer	-0.067 Output
	0 Weights	0.000 Error	0.000 Current Error
PE: 11	1.000 Err Factor	-0.006 Desired	
	-0.006 Sum	-0.006 Transfer	-0.006 Output
	0 Weights	0.000 Error	0.000 Current Error
PE: 12	1.000 Err Factor	-0.233 Desired	
	-0.233 Sum	-0.233 Transfer	-0.233 Output
	0 Weights	0.000 Error	0.000 Current Error
PE: 13	1.000 Err Factor	-0.196 Desired	
	-0.196 Sum	-0.196 Transfer	-0.196 Output
	0 Weights	0.000 Error	0.000 Current Error
PE: 14			

1.000	Err Factor	-0.163	Desired		
-0.163	Sum	-0.163	Transfer	-0.163	Output
0	Weights	0.000	Error	0.000	Current Error
PE: 15					
1.000	Err Factor	-0.210	Desired		
-0.210	Sum	-0.210	Transfer	-0.210	Output
0	Weights	0.000	Error	0.000	Current Error
PE: 16					
1.000	Err Factor	-0.123	Desired		
-0.123	Sum	-0.123	Transfer	-0.123	Output
0	Weights	0.000	Error	0.000	Current Error
PE: 17					
1.000	Err Factor	-0.225	Desired		
-0.225	Sum	-0.225	Transfer	-0.225	Output
0	Weights	0.000	Error	0.000	Current Error
PE: 18					
1.000	Err Factor	-0.086	Desired		
-0.086	Sum	-0.086	Transfer	-0.086	Output
0	Weights	0.000	Error	0.000	Current Error
PE: 19					
1.000	Err Factor	-0.226	Desired		
-0.226	Sum	-0.226	Transfer	-0.226	Output
0	Weights	0.000	Error	0.000	Current Error
PE: 20					
1.000	Err Factor	-0.035	Desired		
-0.035	Sum	-0.035	Transfer	-0.035	Output
0	Weights	0.000	Error	0.000	Current Error
PE: 21					
1.000	Err Factor	-0.223	Desired		
-0.223	Sum	-0.223	Transfer	-0.223	Output
0	Weights	0.000	Error	0.000	Current Error
PE: 22					
1.000	Err Factor	-0.013	Desired		
-0.013	Sum	-0.013	Transfer	-0.013	Output
0	Weights	0.000	Error	0.000	Current Error
PE: 23					
1.000	Err Factor	-0.224	Desired		
-0.224	Sum	-0.224	Transfer	-0.224	Output
0	Weights	0.000	Error	0.000	Current Error
PE: 24					
1.000	Err Factor	0.005	Desired		
0.005	Sum	0.005	Transfer	0.005	Output
0	Weights	0.000	Error	0.000	Current Error
PE: 25					
1.000	Err Factor	-0.225	Desired		
-0.225	Sum	-0.225	Transfer	-0.225	Output
0	Weights	0.000	Error	0.000	Current Error
Layer: Hidden1					
PEs: 18	Wgt Fields: 3	Sum: Sum			
Spacing: 5	F' offset: 0.00	Transfer: TanH			
Shape: Square		Output: Direct			
Scale: 1.00	Low Limit: -9999.00	Error Func: standard			
Offset: 0.00	High Limit: 9999.00	Learn: Norm-Cum-Delta			
Init Low: -0.100	Init High: 0.100	L/R Schedule: hidden1			
Winner 1: None		Winner 2: None			
L/R Schedule: hidden1					

Recall Step	1	0	0	0	0
Input Clamp	0.0000	0.0000	0.0000	0.0000	0.0000
Firing Density	100.0000	0.0000	0.0000	0.0000	0.0000
Temperature	0.0000	0.0000	0.0000	0.0000	0.0000
Gain	1.0000	0.0000	0.0000	0.0000	0.0000
Gain	1.0000	0.0000	0.0000	0.0000	0.0000
Learn Step	10000	30000	70000	150000	310000
Coefficient 1	0.3000	0.1500	0.0375	0.0023	0.0000
Coefficient 2	0.4000	0.2000	0.0500	0.0031	0.0000
Coefficient 3	0.1000	0.1000	0.1000	0.1000	0.1000
Temperature	0.0000	0.0000	0.0000	0.0000	0.0000

PE: 26

1.000 Err Factor	0.000 Desired	
-0.177 Sum	-0.175 Transfer	-0.175 Output
25 Weights	0.000 Error	0.031 Current Error

Input PE	Input Value	Weight	Type	Delta	Weight
Bias	+1.0000	+0.0611	V-r	+0.0002	-0.0013
2	+0.0972	-0.7588	V-r	-0.0002	+0.0003
3	+0.0000	-0.0657	V-r	+0.0000	+0.0000
4	+0.1637	-0.2768	V-r	-0.0000	+0.0001
5	-0.1203	-0.2125	V-r	-0.0000	-0.0002
6	-0.2611	+0.1030	V-r	-0.0000	+0.0007
7	+0.0474	-0.7004	V-r	-0.0000	-0.0004
8	-0.1611	+0.2239	V-r	+0.0001	-0.0001
9	+0.0050	-0.0230	V-r	+0.0001	-0.0001
10	-0.0671	-0.2052	V-r	+0.0001	-0.0003
11	-0.0062	+0.0161	V-r	+0.0002	-0.0002
12	-0.2326	-0.0968	V-r	+0.0001	-0.0000
13	-0.1955	+0.0847	V-r	+0.0001	-0.0001
14	-0.1631	+0.1564	V-r	+0.0001	+0.0000
15	-0.2101	-0.0944	V-r	+0.0001	-0.0002
16	-0.1227	+0.1507	V-r	+0.0001	+0.0001
17	-0.2249	+0.0160	V-r	+0.0001	-0.0001
18	-0.0859	+0.1439	V-r	+0.0001	+0.0001
19	-0.2257	+0.0314	V-r	+0.0001	-0.0001
20	-0.0348	+0.0250	V-r	+0.0000	+0.0001
21	-0.2234	+0.0705	V-r	+0.0001	-0.0002
22	-0.0129	-0.0016	V-r	+0.0000	+0.0002
23	-0.2243	-0.0158	V-r	+0.0001	-0.0001
24	+0.0049	+0.0481	V-r	+0.0000	+0.0002
25	-0.2253	+0.0352	V-r	+0.0001	-0.0001

PE: 27

1.000 Err Factor	0.000 Desired	
0.103 Sum	0.102 Transfer	0.102 Output
25 Weights	0.000 Error	-0.017 Current Error

Input PE	Input Value	Weight	Type	Delta	Weight
Bias	+1.0000	+0.0277	V-r	-0.0001	+0.0006
2	+0.0972	-0.0158	V-r	-0.0001	-0.0002
3	+0.0000	+0.0049	V-r	+0.0000	+0.0000
4	+0.1637	+0.3687	V-r	-0.0001	-0.0001
5	-0.1203	+0.5198	V-r	-0.0000	+0.0001
6	-0.2611	-0.0641	V-r	+0.0000	-0.0003
7	+0.0474	+0.3485	V-r	+0.0000	+0.0002
8	-0.1611	-0.1444	V-r	+0.0001	+0.0001
9	+0.0050	-0.0222	V-r	+0.0001	+0.0000
10	-0.0671	-0.0278	V-r	+0.0000	+0.0003

11	-0.0062	+0.0265	V-r	+0.0002	+0.0003
12	-0.2326	+0.2451	V-r	+0.0001	+0.0002
13	-0.1955	-0.0787	V-r	+0.0002	+0.0001
14	-0.1631	-0.1062	V-r	+0.0000	+0.0001
15	-0.2101	-0.0475	V-r	+0.0002	+0.0002
16	-0.1227	+0.0278	V-r	+0.0000	+0.0001
17	-0.2249	-0.0845	V-r	+0.0002	+0.0001
18	-0.0859	-0.1208	V-r	-0.0000	+0.0000
19	-0.2257	+0.0762	V-r	+0.0002	+0.0001
20	-0.0348	+0.0558	V-r	-0.0000	-0.0000
21	-0.2234	-0.1102	V-r	+0.0002	+0.0001
22	-0.0129	+0.0463	V-r	-0.0001	-0.0000
23	-0.2243	-0.0098	V-r	+0.0001	+0.0001
24	+0.0049	-0.0695	V-r	-0.0001	-0.0001
25	-0.2253	-0.0094	V-r	+0.0001	+0.0001

PE: 28

1.000	Err Factor	0.000	Desired	
-0.087	Sum	-0.087	Transfer	-0.087 Output
25	Weights	0.000	Error	-0.006 Current Error

Input PE	Input Value	Weight	Type	Delta	Weight
Bias	+1.0000	-0.0113	V-r	-0.0003	+0.0005
2	+0.0972	-0.2532	V-r	-0.0001	-0.0000
3	+0.0000	-0.0876	V-r	+0.0000	+0.0000
4	+0.1637	-0.4193	V-r	+0.0001	+0.0000
5	-0.1203	-0.3824	V-r	-0.0001	-0.0001
6	-0.2611	-0.0451	V-r	+0.0001	-0.0000
7	+0.0474	+0.8939	V-r	+0.0001	+0.0001
8	-0.1611	-0.1461	V-r	+0.0000	-0.0001
9	+0.0050	+0.2452	V-r	-0.0002	-0.0002
10	-0.0671	+0.2098	V-r	-0.0001	-0.0001
11	-0.0062	+0.0269	V-r	-0.0003	-0.0001
12	-0.2326	-0.0841	V-r	+0.0000	-0.0001
13	-0.1955	+0.0920	V-r	-0.0002	-0.0000
14	-0.1631	+0.0667	V-r	+0.0001	-0.0001
15	-0.2101	+0.2159	V-r	-0.0002	-0.0000
16	-0.1227	-0.0059	V-r	0.0001	-0.0001
17	-0.2249	+0.1111	V-r	-0.0002	-0.0000
18	-0.0859	-0.1071	V-r	+0.0001	-0.0001
19	-0.2257	+0.1303	V-r	-0.0002	-0.0000
20	-0.0348	-0.0718	V-r	+0.0001	-0.0001
21	-0.2234	-0.0350	V-r	-0.0002	-0.0000
22	-0.0129	-0.1151	V-r	+0.0001	-0.0001
23	-0.2243	+0.0869	V-r	-0.0002	-0.0000
24	+0.0049	-0.1068	V-r	+0.0002	-0.0001
25	-0.2253	-0.0618	V-r	-0.0002	-0.0000

PE: 29

1.000	Err Factor	0.000	Desired	
-0.162	Sum	-0.161	Transfer	-0.161 Output
25	Weights	0.000	Error	0.020 Current Error

Input PE	Input Value	Weight	Type	Delta	Weight
Bias	+1.0000	+0.0644	V-r	-0.0006	-0.0002
2	+0.0972	-0.9245	V-r	-0.0003	-0.0001
3	+0.0000	-0.0526	V-r	+0.0000	+0.0000
4	+0.1637	-0.4824	V-r	+0.0001	-0.0000
5	-0.1203	+0.0926	V-r	-0.0002	-0.0002
6	-0.2611	-0.0419	V-r	+0.0001	+0.0005

7	+0.0474	-0.0209	V-r	+0.0001	-0.0002
8	-0.1611	+0.0419	V-r	+0.0002	-0.0001
9	+0.0050	+0.1004	V-r	-0.0001	-0.0000
10	-0.0671	+0.0505	V-r	+0.0000	+0.0000
11	-0.0062	+0.2302	V-r	-0.0002	-0.0001
12	-0.2326	-0.2007	V-r	+0.0002	+0.0000
13	-0.1955	+0.4118	V-r	-0.0002	-0.0001
14	-0.1631	+0.1284	V-r	+0.0002	+0.0002
15	-0.2101	-0.0790	V-r	-0.0002	-0.0001
16	-0.1227	+0.1414	V-r	+0.0003	+0.0002
17	-0.2249	+0.0292	V-r	-0.0002	-0.0001
18	-0.0859	+0.0259	V-r	+0.0003	+0.0002
19	-0.2257	-0.0960	V-r	-0.0002	-0.0001
20	-0.0348	-0.0650	V-r	+0.0003	+0.0002
21	-0.2234	+0.0479	V-r	-0.0002	-0.0001
22	-0.0129	-0.0095	V-r	+0.0003	+0.0002
23	-0.2243	+0.0646	V-r	-0.0002	-0.0001
24	+0.0049	+0.0985	V-r	+0.0003	+0.0002
25	-0.2253	-0.0855	V-r	-0.0002	-0.0001

PE: 30

1.000	Err Factor	0.000	Desired	
0.183	Sum	0.181	Transfer	0.181 Output
25	Weights	0.000	Error	-0.059 Current Error

Input PE	Input Value	Weight	Type	Delta	Weight
Bias	+1.0000	-0.0744	V-r	-0.0001	+0.0017
2	+0.0972	+0.6242	V-r	+0.0001	-0.0005
3	+0.0000	+0.0973	V-r	+0.0000	+0.0000
4	+0.1637	+0.6067	V-r	-0.0001	-0.0002
5	-0.1203	+0.9707	V-r	+0.0001	+0.0002
6	-0.2611	-0.1894	V-r	+0.0000	-0.0009
7	+0.0474	+0.8321	V-r	+0.0001	+0.0005
8	-0.1611	-0.2452	V-r	+0.0000	+0.0002
9	+0.0050	+0.0978	V-r	+0.0000	+0.0001
10	-0.0671	+0.1108	V-r	-0.0000	+0.0006
11	-0.0062	-0.0512	V-r	+0.0001	+0.0006
12	-0.2326	+0.3010	V-r	-0.0001	+0.0002
13	-0.1955	-0.1205	V-r	+0.0002	+0.0002
14	-0.1631	-0.2714	V-r	-0.0001	+0.0001
15	-0.2101	+0.0850	V-r	+0.0002	+0.0003
16	-0.1227	-0.1242	V-r	-0.0001	-0.0000
17	-0.2249	-0.1035	V-r	+0.0002	+0.0003
18	-0.0859	-0.0810	V-r	-0.0001	-0.0001
19	-0.2257	+0.0009	V-r	+0.0002	+0.0003
20	-0.0348	-0.1227	V-r	-0.0002	-0.0002
21	-0.2234	-0.1296	V-r	+0.0002	+0.0003
22	-0.0129	-0.1172	V-r	-0.0002	-0.0002
23	-0.2243	-0.1031	V-r	+0.0002	+0.0003
24	+0.0049	+0.0662	V-r	-0.0002	-0.0003
25	-0.2253	-0.0411	V-r	+0.0002	+0.0003

PE: 31

1.000	Err Factor	0.000	Desired	
-0.130	Sum	-0.129	Transfer	-0.129 Output
25	Weights	0.000	Error	0.007 Current Error

Input PE	Input Value	Weight	Type	Delta	Weight
Bias	+1.0000	+0.0061	V-r	-0.0001	-0.0003
2	+0.0972	-0.9441	V-r	-0.0003	+0.0000

3	+0.0000	-0.0183	V-r	+0.0000	+0.0000
4	+0.1637	-0.1559	V-r	-0.0000	-0.0000
5	-0.1203	+0.3951	V-r	-0.0001	-0.0002
6	-0.2611	+0.0116	V-r	+0.0000	+0.0003
7	+0.0474	-0.0004	V-r	+0.0001	-0.0001
8	-0.1611	+0.0716	V-r	+0.0002	-0.0000
9	+0.0050	-0.0419	V-r	+0.0001	-0.0001
10	-0.0671	+0.0032	V-r	+0.0001	+0.0001
11	-0.0062	+0.1900	V-r	+0.0001	+0.0001
12	-0.2326	-0.1092	V-r	+0.0002	+0.0001
13	-0.1955	+0.1083	V-r	+0.0001	-0.0000
14	-0.1631	+0.0567	V-r	+0.0002	+0.0001
15	-0.2101	-0.1148	V-r	+0.0001	-0.0000
16	-0.1227	-0.0368	V-r	+0.0001	+0.0001
17	-0.2249	-0.0187	V-r	+0.0001	-0.0000
18	-0.0859	+0.0790	V-r	+0.0001	+0.0001
19	-0.2257	-0.0367	V-r	+0.0001	-0.0000
20	-0.0348	+0.1226	V-r	+0.0001	+0.0001
21	-0.2234	+0.0401	V-r	+0.0001	-0.0000
22	-0.0129	+0.0037	V-r	+0.0001	+0.0001
23	-0.2243	-0.0428	V-r	+0.0001	-0.0000
24	+0.0049	+0.0302	V-r	+0.0001	+0.0001
25	-0.2253	-0.0840	V-r	+0.0001	-0.0000

PE: 32

1.000	Err Factor	0.000	Desired	
0.094	Sum	0.094	Transfer	0.094 Output
25	Weights	0.000	Error	-0.012 Current Error

Input PE	Input Value	Weight	Type	Delta	Weight
Bias	+1.0000	-0.0927	V-r	-0.0004	+0.0006
2	+0.0972	+0.5776	V-r	+0.0002	+0.0000
3	+0.0000	-0.0193	V-r	+0.0000	+0.0000
4	+0.1637	-0.4384	V-r	+0.0001	+0.0000
5	-0.1203	-0.6538	V-r	+0.0000	-0.0000
6	-0.2611	+0.0258	V-r	+0.0000	-0.0001
7	+0.0474	+0.6536	V-r	+0.0000	+0.0001
8	-0.1611	+0.0525	V-r	-0.0002	-0.0000
9	+0.0050	-0.0064	V-r	-0.0002	-0.0001
10	-0.0671	-0.1262	V-r	-0.0002	-0.0002
11	-0.0062	-0.0214	V-r	-0.0005	-0.0002
12	-0.2326	-0.1035	V-r	-0.0001	-0.0002
13	-0.1955	-0.0712	V-r	-0.0003	-0.0001
14	-0.1631	-0.0246	V-r	-0.0000	-0.0002
15	-0.2101	+0.0027	V-r	-0.0003	-0.0000
16	-0.1227	-0.0541	V-r	+0.0000	-0.0002
17	-0.2249	-0.0061	V-r	-0.0003	-0.0000
18	-0.0859	-0.0274	V-r	+0.0001	-0.0002
19	-0.2257	-0.0849	V-r	-0.0003	-0.0000
20	-0.0348	+0.0798	V-r	+0.0001	-0.0001
21	-0.2234	-0.1217	V-r	-0.0003	-0.0000
22	-0.0129	+0.0468	V-r	+0.0002	-0.0001
23	-0.2243	+0.0459	V-r	-0.0003	-0.0000
24	+0.0049	+0.0079	V-r	+0.0002	-0.0001
25	-0.2253	-0.0653	V-r	-0.0003	-0.0000

PE: 33

1.000	Err Factor	0.000	Desired	
0.034	Sum	0.034	Transfer	0.034 Output

25 Weights			0.000 Error		0.001 Current Error
Input PE	Input Value	Weight	Type	Delta Weight	
Bias	+1.0000	+0.0095	V-r	-0.0002	+0.0001
2	+0.0972	+0.4573	V-r	+0.0002	+0.0001
3	+0.0000	-0.0449	V-r	+0.0000	+0.0000
4	+0.1637	-0.5102	V-r	+0.0001	+0.0000
5	-0.1203	-0.5123	V-r	+0.0000	+0.0000
6	-0.2611	-0.0124	V-r	+0.0000	+0.0000
7	+0.0474	+0.2311	V-r	+0.0000	-0.0000
8	-0.1611	+0.3702	V-r	-0.0002	-0.0001
9	+0.0050	-0.0064	V-r	-0.0002	-0.0001
10	-0.0671	-0.0769	V-r	-0.0001	-0.0003
11	-0.0062	+0.1132	V-r	-0.0004	-0.0002
12	-0.2326	-0.2588	V-r	-0.0001	-0.0003
13	-0.1955	-0.0473	V-r	-0.0003	-0.0001
14	-0.1631	+0.0202	V-r	-0.0000	-0.0002
15	-0.2101	+0.0708	V-r	-0.0003	-0.0001
16	-0.1227	+0.0495	V-r	+0.0000	-0.0002
17	-0.2249	+0.0386	V-r	-0.0003	-0.0001
18	-0.0859	+0.0026	V-r	+0.0001	-0.0002
19	-0.2257	+0.0620	V-r	-0.0003	-0.0001
20	-0.0348	-0.1191	V-r	+0.0001	-0.0001
21	-0.2234	-0.0053	V-r	-0.0003	-0.0001
22	-0.0129	+0.0190	V-r	+0.0002	-0.0001
23	-0.2243	-0.0720	V-r	-0.0003	-0.0001
24	+0.0049	-0.0776	V-r	+0.0002	-0.0001
25	-0.2253	+0.0019	V-r	-0.0003	-0.0001

PE: 34

1.000 Err Factor 0.000 Desired

0.952 Sum 0.741 Transfer

0.741 Output

25 Weights

0.000 Error

-0.002 Current Error

Input PE	Input Value	Weight	Type	Delta Weight	
Bias	+1.0000	+0.5603	V-r	+0.0012	-0.0010
2	+0.0972	-1.3688	V-r	-0.0004	+0.0005
3	+0.0000	-0.0904	V-r	+0.0000	+0.0000
4	+0.1637	+1.2547	V-r	-0.0003	+0.0003
5	-0.1203	-1.4151	V-r	-0.0001	-0.0003
6	-0.2611	-0.0042	V-r	-0.0000	+0.0001
7	+0.0474	+1.3175	V-r	-0.0002	+0.0006
8	-0.1611	-0.4817	V-r	+0.0001	-0.0003
9	+0.0050	-0.4277	V-r	+0.0001	-0.0006
10	-0.0671	+0.1326	V-r	+0.0005	-0.0001
11	-0.0062	+0.2977	V-r	+0.0006	+0.0003
12	-0.2326	-0.0239	V-r	+0.0003	-0.0001
13	-0.1955	-0.2903	V-r	+0.0003	-0.0000
14	-0.1631	+0.0715	V-r	+0.0004	-0.0005
15	-0.2101	+0.1189	V-r	+0.0002	+0.0001
16	-0.1227	-0.0275	V-r	+0.0003	-0.0004
17	-0.2249	-0.0534	V-r	+0.0002	+0.0001
18	-0.0859	+0.0232	V-r	+0.0003	-0.0004
19	-0.2257	+0.0046	V-r	+0.0002	+0.0001
20	-0.0348	+0.0203	V-r	+0.0002	-0.0004
21	-0.2234	+0.0413	V-r	+0.0002	+0.0001
22	-0.0129	-0.0526	V-r	+0.0001	-0.0003
23	-0.2243	-0.0075	V-r	+0.0002	+0.0001
24	+0.0049	-0.0035	V-r	-0.0001	-0.0003

25 -0.2253 +0.0411 V-r +0.0002 +0.0001

PE: 35

1.000 Err Factor 0.000 Desired

-0.059 Sum -0.059 Transfer -0.059 Output

25 Weights 0.000 Error -0.003 Current Error

Input PE	Input Value	Weight	Type	Delta	Weight
Bias	+1.0000	-0.0287	V-r	-0.0001	+0.0002
2	+0.0972	-0.1623	V-r	-0.0001	-0.0001
3	+0.0000	-0.0414	V-r	+0.0000	+0.0000
4	+0.1637	+0.2402	V-r	-0.0000	-0.0000
5	-0.1203	+0.1454	V-r	-0.0000	-0.0001
6	-0.2611	+0.0085	V-r	+0.0000	-0.0000
7	+0.0474	+0.1607	V-r	+0.0000	+0.0001
8	-0.1611	-0.1401	V-r	+0.0001	+0.0001
9	+0.0050	-0.0389	V-r	+0.0000	+0.0000
10	-0.0671	-0.1009	V-r	+0.0000	+0.0002
11	-0.0062	-0.0234	V-r	+0.0001	+0.0001
12	-0.2326	+0.1217	V-r	+0.0001	+0.0001
13	-0.1955	-0.1017	V-r	+0.0001	+0.0000
14	-0.1631	+0.0973	V-r	+0.0000	+0.0001
15	-0.2101	+0.0562	V-r	+0.0001	+0.0001
16	-0.1227	+0.0734	V-r	+0.0000	+0.0001
17	-0.2249	+0.0414	V-r	+0.0001	+0.0000
18	-0.0859	+0.1055	V-r	+0.0000	+0.0001
19	-0.2257	-0.0673	V-r	+0.0001	+0.0000
20	-0.0348	-0.0403	V-r	-0.0000	+0.0001
21	-0.2234	+0.0330	V-r	+0.0001	+0.0000
22	-0.0129	+0.0092	V-r	-0.0000	+0.0000
23	-0.2243	-0.0449	V-r	+0.0001	+0.0000
24	+0.0049	-0.0109	V-r	-0.0000	+0.0000
25	-0.2253	+0.1183	V-r	+0.0001	+0.0000

PE: 36

1.000 Err Factor 0.000 Desired

-0.050 Sum -0.050 Transfer -0.050 Output

25 Weights 0.000 Error -0.009 Current Error

Input PE	Input Value	Weight	Type	Delta	Weight
Bias	+1.0000	+0.1406	V-r	-0.0005	+0.0005
2	+0.0972	-0.1425	V-r	-0.0001	-0.0001
3	+0.0000	-0.0008	V-r	+0.0000	+0.0000
4	+0.1637	-0.5744	V-r	+0.0000	-0.0000
5	-0.1203	+0.4702	V-r	-0.0001	-0.0000
6	-0.2611	-0.0486	V-r	+0.0001	-0.0000
7	+0.0474	+0.5094	V-r	+0.0001	+0.0000
8	-0.1611	+0.1720	V-r	+0.0001	+0.0000
9	+0.0050	+0.0168	V-r	-0.0001	-0.0000
10	-0.0671	+0.0535	V-r	-0.0000	+0.0001
11	-0.0062	-0.0204	V-r	-0.0002	+0.0001
12	-0.2326	+0.1140	V-r	+0.0001	+0.0000
13	-0.1955	+0.2612	V-r	-0.0001	+0.0000
14	-0.1631	+0.0511	V-r	+0.0001	+0.0001
15	-0.2101	+0.0149	V-r	-0.0001	+0.0000
16	-0.1227	-0.0967	V-r	+0.0001	+0.0001
17	-0.2249	+0.0032	V-r	-0.0001	+0.0000
18	-0.0859	-0.0233	V-r	+0.0002	+0.0000
19	-0.2257	-0.0519	V-r	-0.0001	+0.0000
20	-0.0348	+0.0797	V-r	+0.0002	+0.0000

21	-0.2234	-0.0047	V-r	-0.0001	+0.0000
22	-0.0129	-0.0712	V-r	+0.0002	+0.0000
23	-0.2243	-0.1158	V-r	-0.0001	+0.0000
24	+0.0049	+0.0066	V-r	+0.0002	-0.0000
25	-0.2253	-0.0317	V-r	-0.0001	+0.0000

PE: 37

1.000	Err Factor	0.000	Desired	
0.129	Sum	0.129	Transfer	0.129 Output
25	Weights	0.000	Error	0.002 Current Error

Input PE	Input Value	Weight	Type	Delta	Weight
Bias	+1.0000	-0.0155	V-r	-0.0002	+0.0002
2	+0.0972	+0.2328	V-r	+0.0001	-0.0000
3	+0.0000	-0.0950	V-r	+0.0000	+0.0000
4	+0.1637	-0.1561	V-r	+0.0001	+0.0000
5	-0.1203	-0.1625	V-r	-0.0000	-0.0000
6	-0.2611	-0.0703	V-r	+0.0000	-0.0000
7	+0.0474	+0.1595	V-r	+0.0000	+0.0000
8	-0.1611	-0.0491	V-r	-0.0001	-0.0000
9	+0.0050	-0.0669	V-r	-0.0001	-0.0000
10	-0.0671	-0.0954	V-r	-0.0001	-0.0000
11	-0.0062	+0.0090	V-r	-0.0002	-0.0001
12	-0.2326	-0.1262	V-r	-0.0000	-0.0001
13	-0.1955	+0.0492	V-r	-0.0001	-0.0000
14	-0.1631	-0.0109	V-r	-0.0000	-0.0000
15	-0.2101	-0.0959	V-r	-0.0001	-0.0000
16	-0.1227	-0.0152	V-r	+0.0000	-0.0000
17	-0.2249	-0.0124	V-r	-0.0001	-0.0000
18	-0.0859	+0.0139	V-r	+0.0000	-0.0000
19	-0.2257	-0.0992	V-r	-0.0001	-0.0000
20	-0.0348	+0.0352	V-r	+0.0001	-0.0000
21	-0.2234	+0.0224	V-r	-0.0001	-0.0000
22	-0.0129	-0.0362	V-r	+0.0001	-0.0000
23	-0.2243	-0.0148	V-r	-0.0001	-0.0000
24	+0.0049	-0.0269	V-r	+0.0001	-0.0000
25	-0.2253	-0.1037	V-r	-0.0001	-0.0000

PE: 38

1.000	Err Factor	0.000	Desired	
-0.073	Sum	-0.073	Transfer	-0.073 Output
25	Weights	0.000	Error	0.007 Current Error

Input PE	Input Value	Weight	Type	Delta	Weight
Bias	+1.0000	+0.1085	V-r	+0.0002	-0.0002
2	+0.0972	-1.2150	V-r	-0.0004	-0.0002
3	+0.0000	-0.0981	V-r	+0.0000	+0.0000
4	+0.1637	+0.6721	V-r	-0.0001	-0.0000
5	-0.1203	+0.9902	V-r	-0.0001	-0.0002
6	-0.2611	+0.1550	V-r	+0.0000	+0.0002
7	+0.0474	-0.3594	V-r	-0.0000	-0.0001
8	-0.1611	-0.3346	V-r	+0.0003	+0.0001
9	+0.0050	+0.1132	V-r	+0.0003	+0.0000
10	-0.0671	-0.2774	V-r	+0.0002	+0.0004
11	-0.0062	-0.3059	V-r	+0.0005	+0.0003
12	-0.2326	+0.1746	V-r	+0.0003	+0.0004
13	-0.1955	+0.1943	V-r	+0.0004	+0.0001
14	-0.1631	-0.1010	V-r	+0.0002	+0.0003
15	-0.2101	-0.0080	V-r	+0.0004	+0.0001
16	-0.1227	-0.1954	V-r	+0.0001	+0.0003

17	-0.2249	+0.0845	V-r	+0.0004	+0.0001
18	-0.0859	+0.0213	V-r	+0.0000	+0.0003
19	-0.2257	+0.0553	V-r	+0.0004	+0.0001
20	-0.0348	-0.0062	V-r	-0.0000	+0.0003
21	-0.2234	+0.0156	V-r	+0.0004	+0.0001
22	-0.0129	+0.0405	V-r	-0.0001	+0.0002
23	-0.2243	+0.0713	V-r	+0.0004	+0.0001
24	+0.0049	-0.0934	V-r	-0.0001	+0.0002
25	-0.2253	-0.0812	V-r	+0.0004	+0.0001

PE: 39

1.000	Err Factor	0.000	Desired	
0.158	Sum	0.157	Transfer	0.157 Output
25	Weights	0.000	Error	0.009 Current Error

Input PE	Input Value	Weight	Type	Delta	Weight
Bias	+1.0000	-0.3298	V-r	+0.0014	-0.0008
2	+0.0972	+1.1721	V-r	+0.0005	+0.0003
3	+0.0000	-0.0493	V-r	+0.0000	+0.0000
4	+0.1637	+0.8559	V-r	-0.0002	+0.0001
5	-0.1203	-0.7835	V-r	+0.0004	+0.0003
6	-0.2611	+0.0644	V-r	-0.0002	-0.0003
7	+0.0474	-1.2694	V-r	-0.0004	-0.0001
8	-0.1611	-0.3613	V-r	-0.0004	-0.0000
9	+0.0050	-0.2047	V-r	+0.0002	+0.0001
10	-0.0671	-0.0621	V-r	+0.0000	-0.0004
11	-0.0062	-0.0286	V-r	+0.0005	-0.0002
12	-0.2326	+0.0013	V-r	-0.0005	-0.0001
13	-0.1955	-0.5125	V-r	+0.0002	-0.0001
14	-0.1631	-0.0471	V-r	-0.0004	-0.0003
15	-0.2101	-0.1716	V-r	+0.0003	-0.0001
16	-0.1227	-0.0329	V-r	-0.0004	-0.0002
17	-0.2249	-0.0874	V-r	+0.0003	-0.0001
18	-0.0859	-0.0018	V-r	-0.0005	-0.0002
19	-0.2257	+0.0273	V-r	+0.0003	-0.0001
20	-0.0348	-0.0070	V-r	-0.0005	-0.0001
21	-0.2234	+0.0144	V-r	+0.0003	-0.0001
22	-0.0129	+0.0379	V-r	-0.0005	-0.0001
23	-0.2243	-0.0087	V-r	+0.0003	-0.0001
24	+0.0049	-0.0812	V-r	-0.0005	-0.0000
25	-0.2253	+0.0183	V-r	+0.0003	-0.0001

PE: 40

1.000	Err Factor	0.000	Desired	
-0.542	Sum	-0.494	Transfer	-0.494 Output
25	Weights	0.000	Error	-0.012 Current Error

Input PE	Input Value	Weight	Type	Delta	Weight
Bias	+1.0000	-0.3236	V-r	-0.0003	+0.0006
2	+0.0972	+0.2620	V-r	+0.0000	-0.0002
3	+0.0000	-0.0907	V-r	+0.0000	+0.0000
4	+0.1637	-0.5094	V-r	+0.0000	-0.0001
5	-0.1203	+0.9148	V-r	-0.0000	+0.0001
6	-0.2611	-0.1067	V-r	+0.0000	-0.0002
7	+0.0474	+0.0534	V-r	+0.0001	-0.0000
8	-0.1611	+0.1075	V-r	+0.0000	+0.0001
9	+0.0050	+0.1570	V-r	-0.0000	+0.0002
10	-0.0671	+0.0063	V-r	-0.0001	+0.0002
11	-0.0062	-0.1388	V-r	-0.0001	+0.0001
12	-0.2326	+0.1803	V-r	-0.0000	+0.0001

13	-0.1955	+0.1035	V-r	-0.0000	+0.0000
14	-0.1631	+0.0268	V-r	-0.0000	+0.0001
15	-0.2101	-0.0737	V-r	-0.0000	+0.0001
16	-0.1227	-0.0881	V-r	-0.0000	+0.0001
17	-0.2249	+0.0449	V-r	-0.0000	+0.0000
18	-0.0859	-0.0015	V-r	-0.0000	+0.0001
19	-0.2257	+0.0514	V-r	-0.0000	+0.0000
20	-0.0348	-0.0957	V-r	-0.0000	+0.0001
21	-0.2234	-0.0577	V-r	-0.0000	+0.0000
22	-0.0129	-0.0063	V-r	-0.0000	+0.0000
23	-0.2243	+0.0353	V-r	-0.0000	+0.0000
24	+0.0049	-0.0592	V-r	+0.0000	+0.0000
25	-0.2253	+0.0481	V-r	-0.0000	+0.0000

PE: 41

1.000	Err Factor	0.000	Desired	
-0.209	Sum	-0.206	Transfer	-0.206 Output
25	Weights	0.000	Error	0.009 Current Error

Input PE	Input Value	Weight	Type	Delta	Weight
Bias	+1.0000	-0.1323	V-r	+0.0009	-0.0009
2	+0.0972	+0.1217	V-r	+0.0000	+0.0003
3	+0.0000	+0.0491	V-r	+0.0000	+0.0000
4	+0.1637	+0.1832	V-r	-0.0002	+0.0001
5	-0.1203	-0.0569	V-r	+0.0002	+0.0001
6	-0.2611	+0.1401	V-r	-0.0001	+0.0001
7	+0.0474	-1.0352	V-r	-0.0002	-0.0002
8	-0.1611	+0.1702	V-r	-0.0001	-0.0001
9	+0.0050	+0.1421	V-r	+0.0002	+0.0000
10	-0.0671	-0.1333	V-r	+0.0001	-0.0002
11	-0.0062	+0.0979	V-r	+0.0004	-0.0000
12	-0.2326	+0.0304	V-r	-0.0001	-0.0001
13	-0.1955	-0.1864	V-r	+0.0003	-0.0000
14	-0.1631	+0.0035	V-r	-0.0001	-0.0002
15	-0.2101	+0.0053	V-r	+0.0003	-0.0000
16	-0.1227	+0.0697	V-r	-0.0002	-0.0002
17	-0.2249	+0.1064	V-r	+0.0003	-0.0000
18	-0.0859	-0.0448	V-r	-0.0002	-0.0001
19	-0.2257	+0.0873	V-r	+0.0003	-0.0000
20	-0.0348	+0.0372	V-r	-0.0002	-0.0001
21	-0.2234	-0.0378	V-r	+0.0003	-0.0000
22	-0.0129	-0.0254	V-r	-0.0002	-0.0001
23	-0.2243	+0.0592	V-r	+0.0003	-0.0000
24	+0.0049	+0.0460	V-r	-0.0003	-0.0000
25	-0.2253	-0.0235	V-r	+0.0003	-0.0000

PE: 42

1.000	Err Factor	0.000	Desired	
0.028	Sum	0.028	Transfer	0.028 Output
25	Weights	0.000	Error	-0.019 Current Error

Input PE	Input Value	Weight	Type	Delta	Weight
Bias	+1.0000	-0.0026	V-r	+0.0002	+0.0004
2	+0.0972	+0.3776	V-r	+0.0000	-0.0002
3	+0.0000	-0.0826	V-r	+0.0000	+0.0000
4	+0.1637	+0.6585	V-r	-0.0001	-0.0001
5	-0.1203	+0.5614	V-r	+0.0001	+0.0001
6	-0.2611	+0.1104	V-r	-0.0001	-0.0004
7	+0.0474	-0.4245	V-r	-0.0000	+0.0001
8	-0.1611	-0.0024	V-r	+0.0001	+0.0001

9	+0.0050	-0.0919	V-r	+0.0002	+0.0002
10	-0.0671	+0.0677	V-r	+0.0000	+0.0003
11	-0.0062	+0.2739	V-r	+0.0004	+0.0003
12	-0.2326	+0.0631	V-r	-0.0001	+0.0002
13	-0.1955	-0.0555	V-r	+0.0003	+0.0001
14	-0.1631	-0.1273	V-r	-0.0001	+0.0001
15	-0.2101	-0.0524	V-r	+0.0003	+0.0002
16	-0.1227	-0.1814	V-r	-0.0002	+0.0001
17	-0.2249	+0.0025	V-r	+0.0003	+0.0001
18	-0.0859	-0.0378	V-r	-0.0002	+0.0001
19	-0.2257	-0.0125	V-r	+0.0003	+0.0001
20	-0.0348	-0.0570	V-r	-0.0003	+0.0000
21	-0.2234	+0.1262	V-r	+0.0003	+0.0001
22	-0.0129	-0.0793	V-r	-0.0003	-0.0000
23	-0.2243	+0.0963	V-r	+0.0003	+0.0001
24	+0.0049	+0.0288	V-r	-0.0003	-0.0000
25	-0.2253	+0.0028	V-r	+0.0003	+0.0001

PE: 43

1.000	Err Factor	0.000	Desired	
-0.062	Sum	-0.062	Transfer	-0.062 Output
25	Weights	0.000	Error	0.010 Current Error

Input PE	Input Value	Weight	Type	Delta	Weight
Bias	+1.0000	-0.0004	V-r	+0.0003	-0.0004
2	+0.0972	+0.1315	V-r	-0.0001	+0.0001
3	+0.0000	-0.0967	V-r	+0.0000	+0.0000
4	+0.1637	+0.0842	V-r	-0.0001	+0.0000
5	-0.1203	+0.3687	V-r	-0.0000	+0.0001
6	-0.2611	-0.0213	V-r	-0.0000	+0.0000
7	+0.0474	-0.7289	V-r	-0.0001	-0.0001
8	-0.1611	-0.1038	V-r	+0.0001	+0.0000
9	+0.0050	-0.0336	V-r	+0.0002	+0.0001
10	-0.0671	+0.1120	V-r	+0.0001	+0.0001
11	-0.0062	+0.1111	V-r	+0.0003	+0.0001
12	-0.2326	+0.0882	V-r	+0.0000	+0.0001
13	-0.1955	+0.0613	V-r	+0.0002	+0.0000
14	-0.1631	-0.1499	V-r	-0.0000	+0.0000
15	-0.2101	-0.0536	V-r	+0.0002	+0.0000
16	-0.1227	-0.0331	V-r	-0.0000	+0.0000
17	-0.2249	+0.1409	V-r	+0.0002	+0.0000
18	-0.0859	-0.1559	V-r	-0.0001	+0.0000
19	-0.2257	-0.0195	V-r	+0.0002	+0.0000
20	-0.0348	+0.0000	V-r	-0.0001	+0.0000
21	-0.2234	+0.0464	V-r	+0.0002	+0.0000
22	-0.0129	-0.1297	V-r	-0.0001	+0.0000
23	-0.2243	+0.0322	V-r	+0.0002	+0.0000
24	+0.0049	-0.0724	V-r	-0.0001	+0.0000
25	-0.2253	+0.0003	V-r	+0.0002	+0.0000

Layer: Hidden2

PEs: 12	Wgt Fields: 3	Sum: Sum
Spacing: 5	F' offset: 0.00	Transfer: TanH
Shape: Square		Output: Direct
Scale: 1.00	Low Limit: -9999.00	Error Func: standard
Offset: 0.00	High Limit: 9999.00	Learn: Norm-Cum-Delta
Init Low: -0.100	Init High: 0.100	L/R Schedule: hidden2
Winner 1: None		Winner 2: None
L/R Schedule: hidden2		

Recall Step	1	0	0	0	0
Input Clamp	0.0000	0.0000	0.0000	0.0000	0.0000
Firing Density	100.0000	0.0000	0.0000	0.0000	0.0000
Temperature	0.0000	0.0000	0.0000	0.0000	0.0000
Gain	1.0000	0.0000	0.0000	0.0000	0.0000
Gain	1.0000	0.0000	0.0000	0.0000	0.0000
Learn Step	10000	30000	70000	150000	310000
Coefficient 1	0.2500	0.1250	0.0312	0.0020	0.0000
Coefficient 2	0.4000	0.2000	0.0500	0.0031	0.0000
Coefficient 3	0.1000	0.1000	0.1000	0.1000	0.1000
Temperature	0.0000	0.0000	0.0000	0.0000	0.0000

PE: 44

1.000 Err Factor	0.000 Desired	
-0.290 Sum	-0.282 Transfer	-0.282 Output
19 Weights	0.000 Error	0.012 Current Error

Input PE	Input Value	Weight	Type	Delta	Weight
Bias	+1.0000	-0.2609	V-r	-0.0002	+0.0001
26	-0.1752	-0.0605	V-r	+0.0001	+0.0001
27	+0.1022	-0.0771	V-r	-0.0000	-0.0001
28	-0.0872	-0.0317	V-r	-0.0001	+0.0000
29	-0.1610	-0.1372	V-r	+0.0000	+0.0001
30	+0.1813	-0.0849	V-r	-0.0002	-0.0001
31	-0.1294	-0.0927	V-r	+0.0000	+0.0000
32	+0.0935	+0.1280	V-r	-0.0000	-0.0000
33	+0.0338	-0.0314	V-r	-0.0000	-0.0000
34	+0.7408	-0.1983	V-r	+0.0001	+0.0000
35	-0.0589	+0.0714	V-r	+0.0000	-0.0000
36	-0.0499	-0.0362	V-r	-0.0001	-0.0000
37	+0.1285	+0.1304	V-r	-0.0000	-0.0000
38	-0.0728	-0.2312	V-r	+0.0000	-0.0001
39	+0.1570	-0.0794	V-r	+0.0001	-0.0001
40	-0.4944	-0.1091	V-r	-0.0001	-0.0001
41	-0.2056	-0.0706	V-r	+0.0001	-0.0000
42	+0.0276	-0.0777	V-r	-0.0000	-0.0001
43	-0.0617	+0.0416	V-r	-0.0000	-0.0000

PE: 45

1.000 Err Factor	0.000 Desired	
-0.358 Sum	-0.343 Transfer	-0.343 Output
19 Weights	0.000 Error	0.038 Current Error

Input PE	Input Value	Weight	Type	Delta	Weight
Bias	+1.0000	+0.2012	V-r	+0.0003	-0.0004
26	-0.1752	+0.4681	V-r	+0.0003	+0.0002
27	+0.1022	+0.2028	V-r	-0.0001	-0.0001
28	-0.0872	-0.6587	V-r	+0.0003	-0.0000
29	-0.1610	+0.2028	V-r	+0.0005	+0.0001
30	+0.1813	-0.0043	V-r	-0.0004	-0.0002
31	-0.1294	+0.4720	V-r	+0.0003	+0.0001
32	+0.0935	-0.9218	V-r	-0.0003	-0.0001
33	+0.0338	-0.6874	V-r	+0.0001	-0.0001
34	+0.7408	-0.0896	V-r	+0.0002	-0.0001
35	-0.0589	+0.1659	V-r	-0.0000	+0.0000
36	-0.0499	-0.1287	V-r	+0.0002	-0.0001
37	+0.1285	-0.2855	V-r	-0.0002	-0.0001
38	-0.0728	+1.2800	V-r	+0.0002	-0.0001
39	+0.1570	-0.0045	V-r	-0.0005	+0.0001
40	-0.4944	+0.0906	V-r	-0.0000	+0.0001

41	-0.2056	+0.4336	V-r	+0.0000	+0.0002
42	+0.0276	+0.4943	V-r	+0.0000	-0.0000
43	-0.0617	+0.4917	V-r	+0.0001	+0.0000
PE: 46					
1.000	Err Factor	0.000	Desired		
-0.029	Sum	-0.029	Transfer		-0.029 Output
19	Weights	0.000	Error		-0.006 Current Error
Input PE	Input Value	Weight	Type	Delta	Weight
Bias	+1.0000	+0.2452	V-r	-0.0004	+0.0004
26	-0.1752	-0.1542	V-r	-0.0002	+0.0005
27	+0.1022	-0.0220	V-r	+0.0001	-0.0002
28	-0.0872	+0.0831	V-r	+0.0000	+0.0000
29	-0.1610	+0.0608	V-r	-0.0001	+0.0004
30	+0.1813	-0.0894	V-r	+0.0002	-0.0005
31	-0.1294	-0.0666	V-r	-0.0001	+0.0003
32	+0.0935	+0.0995	V-r	+0.0000	-0.0001
33	+0.0338	-0.0258	V-r	-0.0000	-0.0001
34	+0.7408	-0.5309	V-r	-0.0002	+0.0002
35	-0.0589	+0.0003	V-r	+0.0000	+0.0001
36	-0.0499	-0.1625	V-r	-0.0001	+0.0001
37	+0.1285	-0.0187	V-r	+0.0000	-0.0001
38	-0.0728	-0.0727	V-r	+0.0000	+0.0001
39	+0.1570	+0.2676	V-r	+0.0001	-0.0003
40	-0.4944	-0.0703	V-r	+0.0002	-0.0003
41	-0.2056	-0.0848	V-r	-0.0000	-0.0000
42	+0.0276	+0.0660	V-r	+0.0001	-0.0005
43	-0.0617	-0.0610	V-r	+0.0000	-0.0003
PE: 47					
1.000	Err Factor	0.000	Desired		
0.394	Sum	0.375	Transfer		0.375 Output
19	Weights	0.000	Error		-0.182 Current Error
Input PE	Input Value	Weight	Type	Delta	Weight
Bias	+1.0000	-0.0991	V-r	-0.0001	+0.0010
26	-0.1752	-1.0093	V-r	-0.0001	-0.0000
27	+0.1022	+0.6134	V-r	-0.0000	+0.0002
28	-0.0872	+0.0122	V-r	+0.0001	+0.0005
29	-0.1610	-0.6561	V-r	+0.0000	+0.0004
30	+0.1813	+1.4748	V-r	+0.0001	+0.0001
31	-0.1294	-0.3265	V-r	-0.0001	+0.0003
32	+0.0935	+0.0468	V-r	+0.0000	-0.0002
33	+0.0338	-0.2149	V-r	+0.0001	-0.0000
34	+0.7408	-0.0183	V-r	-0.0002	+0.0008
35	-0.0589	+0.1515	V-r	-0.0000	+0.0000
36	-0.0499	+0.1647	V-r	+0.0001	+0.0005
37	+0.1285	-0.0118	V-r	+0.0000	-0.0001
38	-0.0728	+0.1552	V-r	-0.0000	+0.0001
39	+0.1570	-0.1231	V-r	-0.0001	-0.0010
40	-0.4944	+0.3833	V-r	+0.0001	-0.0001
41	-0.2056	-0.3810	V-r	-0.0000	-0.0005
42	+0.0276	+0.6198	V-r	+0.0001	-0.0002
43	-0.0617	+0.0107	V-r	+0.0001	-0.0001
PE: 48					
1.000	Err Factor	0.000	Desired		
-0.401	Sum	-0.381	Transfer		-0.381 Output
19	Weights	0.000	Error		0.055 Current Error
Input PE	Input Value	Weight	Type	Delta	Weight

Bias	+1.0000	-0.5147	V-r	+0.0001	-0.0007
26	-0.1752	-0.1657	V-r	+0.0003	-0.0003
27	+0.1022	+0.0537	V-r	-0.0001	+0.0001
28	-0.0872	+0.0958	V-r	-0.0001	-0.0000
29	-0.1610	-0.0717	V-r	+0.0001	-0.0003
30	+0.1813	+0.0073	V-r	-0.0003	+0.0004
31	-0.1294	-0.1780	V-r	+0.0001	-0.0002
32	+0.0935	-0.0202	V-r	-0.0000	+0.0000
33	+0.0338	+0.1267	V-r	+0.0000	-0.0000
34	+0.7408	+0.0497	V-r	+0.0003	-0.0004
35	-0.0589	-0.1196	V-r	-0.0000	+0.0000
36	-0.0499	+0.0540	V-r	-0.0001	-0.0001
37	+0.1285	+0.0515	V-r	-0.0000	+0.0001
38	-0.0728	-0.0481	V-r	-0.0000	-0.0000
39	+0.1570	-0.0009	V-r	+0.0001	+0.0002
40	-0.4944	-0.0075	V-r	-0.0002	+0.0003
41	-0.2056	-0.0172	V-r	+0.0001	+0.0001
42	+0.0276	-0.0784	V-r	-0.0001	+0.0003
43	-0.0617	+0.1161	V-r	-0.0001	+0.0002

PE: 49

1.000	Err Factor	0.000	Desired	
0.003	Sum	0.003	Transfer	0.003 Output
19	Weights	0.000	Error	-0.011 Current Error

Input PE	Input Value	Weight	Type	Delta	Weight
Bias	+1.0000	+0.2722	V-r	-0.0004	+0.0004
26	-0.1752	+0.0473	V-r	+0.0001	+0.0002
27	+0.1022	-0.0439	V-r	-0.0000	-0.0001
28	-0.0872	+0.1183	V-r	+0.0000	+0.0001
29	-0.1610	+0.3763	V-r	+0.0000	+0.0002
30	+0.1813	-0.0238	V-r	-0.0001	-0.0003
31	-0.1294	+0.1396	V-r	+0.0001	+0.0001
32	+0.0935	+0.1183	V-r	+0.0001	-0.0000
33	+0.0338	+0.0142	V-r	-0.0000	+0.0000
34	+0.7408	-0.0385	V-r	+0.0001	+0.0002
35	-0.0589	-0.1025	V-r	+0.0000	+0.0000
36	-0.0499	+0.2943	V-r	-0.0001	+0.0000
37	+0.1285	+0.0100	V-r	-0.0000	-0.0000
38	-0.0728	+0.2679	V-r	-0.0000	-0.0001
39	+0.1570	-0.8208	V-r	+0.0000	-0.0002
40	-0.4944	+0.0640	V-r	+0.0000	-0.0002
41	-0.2056	-0.1775	V-r	+0.0000	-0.0000
42	+0.0276	-0.1846	V-r	-0.0001	-0.0002
43	-0.0617	-0.1596	V-r	-0.0001	-0.0001

PE: 50

1.000	Err Factor	0.000	Desired	
-0.468	Sum	-0.436	Transfer	-0.436 Output
19	Weights	0.000	Error	-0.001 Current Error

Input PE	Input Value	Weight	Type	Delta	Weight
Bias	+1.0000	-0.2937	V-r	-0.0001	+0.0001
26	-0.1752	+0.0669	V-r	+0.0002	-0.0002
27	+0.1022	-0.0248	V-r	-0.0001	+0.0000
28	-0.0872	-0.1731	V-r	-0.0001	-0.0000
29	-0.1610	+0.0287	V-r	-0.0000	-0.0002
30	+0.1813	-0.0458	V-r	-0.0002	+0.0002
31	-0.1294	+0.0956	V-r	+0.0000	-0.0002
32	+0.0935	-0.0469	V-r	+0.0000	+0.0000

33	+0.0338	-0.0786	V-r	-0.0000	+0.0000
34	+0.7408	-0.0079	V-r	+0.0000	-0.0001
35	-0.0589	-0.0242	V-r	-0.0000	-0.0001
36	-0.0499	-0.0250	V-r	-0.0001	-0.0001
37	+0.1285	+0.0201	V-r	-0.0000	+0.0001
38	-0.0728	+0.1834	V-r	-0.0001	-0.0001
39	+0.1570	-0.2372	V-r	+0.0001	+0.0002
40	-0.4944	+0.1018	V-r	-0.0001	+0.0000
41	-0.2056	+0.1835	V-r	+0.0001	+0.0001
42	+0.0276	+0.1495	V-r	-0.0001	+0.0002
43	-0.0617	+0.1207	V-r	-0.0000	+0.0002

PE: 51

1.000	Err Factor	0.000	Desired	
-0.074	Sum	-0.074	Transfer	-0.074 Output
19	Weights	0.000	Error	0.015 Current Error

Input PE	Input Value	Weight	Type	Delta	Weight
Bias	+1.0000	-0.2572	V-r	+0.0004	-0.0006
26	-0.1752	-0.0593	V-r	+0.0002	-0.0005
27	+0.1022	-0.0778	V-r	-0.0001	+0.0002
28	-0.0872	-0.0844	V-r	-0.0000	-0.0001
29	-0.1610	-0.0040	V-r	+0.0001	-0.0004
30	+0.1813	-0.0034	V-r	-0.0002	+0.0006
31	-0.1294	-0.0179	V-r	+0.0001	-0.0003
32	+0.0935	-0.0658	V-r	-0.0000	+0.0001
33	+0.0338	+0.0213	V-r	+0.0000	+0.0000
34	+0.7408	+0.3864	V-r	+0.0002	-0.0003
35	-0.0589	-0.0715	V-r	-0.0000	-0.0000
36	-0.0499	+0.0269	V-r	+0.0001	-0.0001
37	+0.1285	-0.1040	V-r	-0.0000	+0.0001
38	-0.0728	-0.0016	V-r	-0.0000	-0.0001
39	+0.1570	+0.1681	V-r	-0.0001	+0.0004
40	-0.4944	+0.1988	V-r	-0.0002	+0.0003
41	-0.2056	+0.0966	V-r	+0.0000	+0.0001
42	+0.0276	-0.0068	V-r	-0.0001	+0.0005
43	-0.0617	+0.1150	V-r	-0.0000	+0.0003

PE: 52

1.000	Err Factor	0.000	Desired	
-0.202	Sum	-0.199	Transfer	-0.199 Output
19	Weights	0.000	Error	0.010 Current Error

Input PE	Input Value	Weight	Type	Delta	Weight
Bias	+1.0000	+0.2434	V-r	-0.0007	+0.0004
26	-0.1752	+0.0401	V-r	+0.0002	+0.0002
27	+0.1022	+0.1606	V-r	-0.0000	-0.0001
28	-0.0872	+0.3984	V-r	-0.0000	+0.0001
29	-0.1610	+0.6213	V-r	+0.0000	+0.0002
30	+0.1813	+0.0992	V-r	-0.0002	-0.0003
31	-0.1294	+0.3901	V-r	+0.0002	+0.0002
32	+0.0935	+0.0323	V-r	+0.0002	-0.0000
33	+0.0338	+0.0890	V-r	-0.0001	+0.0000
34	+0.7408	-0.1021	V-r	+0.0004	+0.0002
35	-0.0589	+0.1418	V-r	+0.0001	+0.0000
36	-0.0499	+0.4590	V-r	-0.0001	+0.0001
37	+0.1285	+0.0099	V-r	-0.0000	-0.0001
38	-0.0728	+0.2529	V-r	-0.0001	-0.0000
39	+0.1570	-1.2595	V-r	+0.0000	-0.0003
40	-0.4944	+0.2073	V-r	-0.0001	-0.0002

41	-0.2056	-0.6387	V-r	-0.0000	-0.0001
42	+0.0276	-0.3318	V-r	-0.0003	-0.0002
43	-0.0617	-0.1358	V-r	-0.0004	-0.0001
PE: 53					
1.000	Err Factor	0.000	Desired		
-0.871	Sum	-0.702	Transfer	-0.702	Output
19	Weights	0.000	Error	-0.009	Current Error
Input PE	Input Value	Weight	Type	Delta	Weight
Bias	+1.0000	-0.0353	V-r	-0.0002	+0.0001
26	-0.1752	-0.0766	V-r	-0.0002	+0.0003
27	+0.1022	-0.1824	V-r	+0.0001	-0.0001
28	-0.0872	-0.0714	V-r	+0.0000	-0.0000
29	-0.1610	+0.0523	V-r	-0.0001	+0.0003
30	+0.1813	-0.0259	V-r	+0.0002	-0.0003
31	-0.1294	-0.0486	V-r	-0.0001	+0.0002
32	+0.0935	-0.1102	V-r	+0.0001	-0.0001
33	+0.0338	+0.1646	V-r	+0.0000	-0.0000
34	+0.7408	-0.9197	V-r	-0.0002	-0.0001
35	-0.0589	-0.0841	V-r	+0.0000	+0.0000
36	-0.0499	+0.0581	V-r	-0.0000	+0.0001
37	+0.1285	-0.0631	V-r	+0.0000	-0.0001
38	-0.0728	-0.0550	V-r	-0.0000	+0.0001
39	+0.1570	+0.1744	V-r	+0.0001	-0.0002
40	-0.4944	+0.2998	V-r	+0.0002	-0.0000
41	-0.2056	+0.0918	V-r	-0.0001	+0.0000
42	+0.0276	+0.1270	V-r	+0.0001	-0.0003
43	-0.0617	+0.0949	V-r	+0.0000	-0.0001
PE: 54					
1.000	Err Factor	0.000	Desired		
0.464	Sum	0.433	Transfer	0.433	Output
19	Weights	0.000	Error	-0.033	Current Error
Input PE	Input Value	Weight	Type	Delta	Weight
Bias	+1.0000	+0.1748	V-r	+0.0004	+0.0001
26	-0.1752	+0.0331	V-r	+0.0000	-0.0001
27	+0.1022	-0.0798	V-r	-0.0000	+0.0001
28	-0.0872	+0.0980	V-r	+0.0001	-0.0000
29	-0.1610	-0.0579	V-r	+0.0001	-0.0002
30	+0.1813	+0.2268	V-r	-0.0000	+0.0001
31	-0.1294	+0.0035	V-r	+0.0000	-0.0001
32	+0.0935	+0.1345	V-r	-0.0001	-0.0000
33	+0.0338	+0.2416	V-r	+0.0000	+0.0000
34	+0.7408	+0.3712	V-r	-0.0001	+0.0002
35	-0.0589	-0.1216	V-r	-0.0001	-0.0000
36	-0.0499	+0.1315	V-r	+0.0002	-0.0000
37	+0.1285	-0.0421	V-r	-0.0000	+0.0000
38	-0.0728	-0.3661	V-r	-0.0000	-0.0000
39	+0.1570	-0.0128	V-r	-0.0003	+0.0002
40	-0.4944	+0.0173	V-r	+0.0000	-0.0000
41	-0.2056	+0.2121	V-r	-0.0000	+0.0000
42	+0.0276	-0.1212	V-r	-0.0000	+0.0002
43	-0.0617	-0.0245	V-r	+0.0001	+0.0002
PE: 55					
1.000	Err Factor	0.000	Desired		
1.320	Sum	0.867	Transfer	0.867	Output
19	Weights	0.000	Error	-0.009	Current Error
Input PE	Input Value	Weight	Type	Delta	Weight

Bias	+1.0000	+0.0474	V-r	+0.0004	-0.0003
26	-0.1752	-0.0786	V-r	+0.0002	-0.0003
27	+0.1022	+0.0996	V-r	-0.0001	+0.0001
28	-0.0872	+0.3329	V-r	+0.0001	+0.0001
29	-0.1610	-0.0436	V-r	+0.0002	-0.0003
30	+0.1813	+0.1183	V-r	-0.0002	+0.0003
31	-0.1294	+0.1815	V-r	+0.0001	-0.0003
32	+0.0935	+0.0224	V-r	-0.0001	+0.0002
33	+0.0338	-0.0559	V-r	-0.0000	+0.0001
34	+0.7408	+1.4368	V-r	+0.0002	+0.0002
35	-0.0589	+0.1276	V-r	-0.0000	+0.0000
36	-0.0499	-0.1603	V-r	+0.0001	-0.0001
37	+0.1285	-0.1070	V-r	-0.0001	+0.0001
38	-0.0728	+0.1622	V-r	+0.0000	-0.0003
39	+0.1570	-0.1270	V-r	-0.0002	+0.0002
40	-0.4944	-0.4368	V-r	-0.0001	+0.0000
41	-0.2056	-0.1298	V-r	+0.0000	-0.0001
42	+0.0276	-0.1359	V-r	-0.0001	+0.0001
43	-0.0617	-0.2358	V-r	+0.0000	-0.0000

Layer: Out

PEs: 4	Wgt Fields: 3	Sum: Sum
Spacing: 5	F' offset: 0.00	Transfer: TanH
Shape: Square		Output: Direct
Scale: 1.00	Low Limit: -9999.00	Error Func: standard
Offset: 0.00	High Limit: 9999.00	Learn: Norm-Cum-Delta
Init Low: -0.100	Init High: 0.100	L/R Schedule: out
Winner 1: None		Winner 2: None

L/R Schedule: out

Recall Step	1	0	0	0	0
Input Clamp	0.0000	0.0000	0.0000	0.0000	0.0000
Firing Density	100.0000	0.0000	0.0000	0.0000	0.0000
Temperature	0.0000	0.0000	0.0000	0.0000	0.0000
Gain	1.0000	0.0000	0.0000	0.0000	0.0000
Gain	1.0000	0.0000	0.0000	0.0000	0.0000
Learn Step	10000	30000	70000	150000	310000
Coefficient 1	0.1500	0.0750	0.0188	0.0012	0.0000
Coefficient 2	0.4000	0.2000	0.0500	0.0031	0.0000
Coefficient 3	0.1000	0.1000	0.1000	0.1000	0.1000
Temperature	0.0000	0.0000	0.0000	0.0000	0.0000

PE: 56

1.000 Err Factor	0.500 Desired	
1.597 Sum	0.921 Transfer	0.921 Output
13 Weights	-0.421 Error	0.013 Current Error

Input PE	Input Value	Weight	Type	Delta	Weight
Bias	+1.0000	+1.1569	V-r	+0.0008	-0.0007
44	-0.2823	-0.2765	V-r	-0.0002	+0.0002
45	-0.3431	+0.0471	V-r	-0.0003	+0.0002
46	-0.0287	-0.0395	V-r	+0.0001	-0.0000
47	+0.3751	-0.0202	V-r	+0.0006	+0.0007
48	-0.3810	-0.2206	V-r	-0.0003	+0.0004
49	+0.0031	-0.4191	V-r	+0.0004	-0.0006
50	-0.4364	-0.1882	V-r	-0.0002	+0.0002
51	-0.0735	+0.0784	V-r	-0.0003	+0.0002
52	-0.1994	-1.0586	V-r	+0.0004	-0.0007
53	-0.7020	+0.1638	V-r	+0.0001	+0.0001
54	+0.4333	+0.2462	V-r	+0.0001	-0.0002

55 +0.8669 +0.0261 V-r -0.0001 -0.0001

PE: 57

1.000	Err Factor	0.500	Desired	
1.728	Sum	0.939	Transfer	0.939 Output
13	Weights	-0.439	Error	-0.032 Current Error

Input PE	Input Value	Weight	Type	Delta	Weight
Bias	+1.0000	+1.1882	V-r	-0.0006	+0.0005
44	-0.2823	-0.0851	V-r	+0.0003	-0.0002
45	-0.3431	-1.3689	V-r	-0.0006	+0.0002
46	-0.0287	+0.0385	V-r	+0.0003	+0.0001
47	+0.3751	+0.0129	V-r	+0.0010	-0.0000
48	-0.3810	-0.1777	V-r	+0.0004	-0.0003
49	+0.0031	-0.0541	V-r	-0.0006	+0.0002
50	-0.4364	+0.0823	V-r	-0.0000	+0.0000
51	-0.0735	-0.0270	V-r	+0.0001	-0.0002
52	-0.1994	+0.0248	V-r	-0.0006	+0.0001
53	-0.7020	+0.0035	V-r	+0.0004	+0.0001
54	+0.4333	+0.0026	V-r	-0.0001	-0.0001
55	+0.8669	+0.0172	V-r	-0.0005	-0.0001

PE: 58

1.000	Err Factor	0.500	Desired	
0.107	Sum	0.106	Transfer	0.106 Output
13	Weights	0.394	Error	0.003 Current Error

Input PE	Input Value	Weight	Type	Delta	Weight
Bias	+1.0000	+1.1699	V-r	-0.0005	+0.0005
44	-0.2823	+0.0315	V-r	+0.0001	-0.0002
45	-0.3431	+0.0099	V-r	-0.0001	+0.0000
46	-0.0287	+0.4051	V-r	+0.0001	-0.0002
47	+0.3751	+0.0035	V-r	+0.0004	-0.0008
48	-0.3810	-0.1546	V-r	+0.0002	-0.0004
49	+0.0031	+0.0697	V-r	-0.0002	+0.0007
50	-0.4364	-0.2602	V-r	+0.0001	-0.0000
51	-0.0735	-0.3034	V-r	+0.0001	-0.0002
52	-0.1994	+0.0620	V-r	-0.0001	+0.0006
53	-0.7020	+0.4614	V-r	+0.0003	-0.0003
54	+0.4333	-0.3215	V-r	-0.0002	-0.0000
55	+0.8669	-0.8766	V-r	-0.0004	+0.0001

PE: 59

1.000	Err Factor	0.500	Desired	
1.884	Sum	0.955	Transfer	0.955 Output
13	Weights	-0.455	Error	-0.129 Current Error

Input PE	Input Value	Weight	Type	Delta	Weight
Bias	+1.0000	+1.0705	V-r	-0.0004	+0.0016
44	-0.2823	-0.0691	V-r	+0.0001	-0.0005
45	-0.3431	+0.0467	V-r	-0.0001	-0.0002
46	-0.0287	+0.0490	V-r	+0.0000	-0.0003
47	+0.3751	+1.4355	V-r	+0.0004	-0.0011
48	-0.3810	-0.3939	V-r	+0.0002	-0.0008
49	+0.0031	+0.1016	V-r	+0.0001	+0.0007
50	-0.4364	-0.0164	V-r	+0.0002	-0.0004
51	-0.0735	-0.1213	V-r	+0.0000	-0.0003
52	-0.1994	-0.0838	V-r	+0.0002	+0.0006
53	-0.7020	+0.0813	V-r	+0.0003	-0.0008
54	+0.4333	+0.2545	V-r	-0.0001	+0.0004
55	+0.8669	+0.0422	V-r	-0.0003	+0.0009

LIST OF REFERENCES

- [1] NUWES Briefing, Bangor Naval Submarine Base, Bangor, Wa., Sept. 1990
- [2] Patrick K. Simpson, *Artificial Neural Systems Foundations, Paradigms, Applications, and Implementations*, Pergamon Press, New York, NY, pp. 100-133, 1990
- [3] M.W. Roth, "Neural networks for extraction of weak targets in high clutter environments," *IJCNN: International Joint Conference on Neural Networks*, Washington, DC, USA, 18-22 June 1989, (New York, N.Y., USA: IEEE TAB Neural Network Committee 1989), vol. 1, pp. 225-232
- [4] A. Khotanzad, J.H. Lu, and M.D. Srinath, "Target Detection using a neural network based passive system," *IJCNN: International Joint Conference on Neural Networks*, Washington, DC, USA, 18-22 June 1989, (New York, NY, USA: IEEE TAB Neural Network Committee 1989), vol. 1, pp. 335-340
- [5] Gustavo de Veciana and Avidesh Zakhori, "Neural net based continuous phase modulation receivers", *Supercomm ICC'90 Conference Record*, Atlanta, Ga., 16-19 April 1990, vol 2, pp. 419-23
- [6] Robert Hecht-Nielsen, *Neurocomputing*, Addison-Wesley Publishing Company, Reading, Ma., 1990
- [7] Gail A. Carpenter, "Neural network models for pattern recognition and associative memory" in *Pattern Recognition by Self-Organizing Neural Networks*, Gail A. Carpenter and Stephen Grossberg, eds, pp. 1-34, The MIT Press, Cambridge, Ma., 1991
- [8] *Neural Computing*, NeuralWare, Inc., pp. NC-89-NC-110, 1991
- [9] Robert J. Urick, *Principles of Underwater Sound*, 3rd edition, McGraw-Hill Book Company, 1983
- [10] Clarence S. Clay, and Herman Medwin, *Acoustical Oceanography: Principles and Applications*, John Wiley & Sons, New York, NY, 1977
- [11] Leon W. Couch II, *Digital and Analog Communication Systems*, 3rd edition, Macmillan Publishing Company, New York, N.Y., 1990

INITIAL DISTRIBUTION LIST

	No. Copies
1. Defense Technical Information Center Cameron Station Alexandria, Virginia 22304-6145	2
2. Library, Code 52 Naval Postgraduate School Monterey, California 93943-5000	2
3. Chairman, Code EC Department of Electrical and Computer Engineering Naval Postgraduate School Monterey, California 93943-5000	1
4. Professor Murali Tummala, Code EC/Tu Department of Electrical and Computer Engineering Naval Postgraduate School Monterey, California 93943-5000	4
5. Professor Harold A. Titus, Code EC-Ts Department of Electrical and Computer Engineering Naval Postgraduate School Monterey, California 93943-5000	1
6. Professor Charles W. Therrien, Code EC/Ti Department of Electrical and Computer Engineering Naval Postgraduate School Monterey, California 93943-5000	1
7. Mr. John Hager (Code 70E1) Naval Undersea Warfare Engineering Station Keyport, Washington 98345	1

- | | | |
|----|--|---|
| 8. | Dr. R. Madan (Code 1114SE)
Office of Naval Research
800 North Quincy Street
Arlington, Virginia 22217 | 1 |
| 9. | Lt. Charles H. Wellington Jr.
1047-A Highland Street
Seaside, California 93955 | 2 |